

www.cpwr.com • www.elcosh.org



Field Tool for On-Site Biomechanical Analysis During Ladder Climbing

SangHyun Lee, PhD

Thomas J. Armstrong, PhD

April 2014

8484 Georgia Avenue
Suite 1000
Silver Spring, MD 20910

PHONE: 301.578.8500

FAX: 301.578.8572



© 2014, CPWR – The Center for Construction Research and Training. CPWR, the research and training arm of the Building and Construction Trades Dept., AFL-CIO, is uniquely situated to serve construction workers, contractors, practitioners, and the scientific community. This report was prepared by the authors noted. Funding for this research study was made possible by a cooperative agreement with the National Institute for Occupational Safety and Health, NIOSH (OH009762). The contents are solely the responsibility of the authors and do not necessarily represent the official views of NIOSH or CPWR.

Field Tool for On-Site Biomechanical Analysis During Ladder Climbing

CPWR Final Report

SangHyun Lee, PhD

Assistant Professor

John L. Tishman CM Faculty Scholar

Department of Civil and Environmental Engineering
University of Michigan

Thomas J. Armstrong, PhD

Professor

Department of Industrial and Operations Engineering
Department of Biomedical Engineering
Director of Center for Ergonomics
University of Michigan

Key Findings of the Study

- Computer vision–based motion capture approaches have a great potential to provide 3D skeleton–based motion data to be used for on-site biomechanical analysis during ladder climbing. In our test, their accuracy is 6.3 cm of average errors in body segment lengths and 6.8 cm of average errors in the 3D positions of body joints.
- External force patterns (hand and foot forces) during ladder climbing are similar under the same individual (i.e., working postures) and physical factors (i.e., working conditions). Thus, external forces under real conditions can be estimated by modeling representative data samples that reflect specific individual and physical factors from laboratory experiments.
- The human skeleton–based motion data extracted from vision-based motion capture approaches are not readily applicable to existing computerized biomechanical analysis tools such as 3D SSPPTM and OpenSim because of compatibility issues in body models of the motion data and computerized biomechanical analysis tools. To address this issue, we developed automated motion data processing to convert vision-based motion data into available file formats that can be directly used in 3D SSPPTM and OpenSim. The proposed motion data processing has been verified and validated successfully, being applied to static and dynamic biomechanical analyses.
- During ladder climbing activities, upper extremities are the most hazardous body parts because of the excessive joint moments generated at wrists and elbows. It is suggested that interventions to reduce musculoskeletal stresses on upper extremities be implemented to prevent ladder-related injuries.
- Hands are the most difficult body parts to track using vision-based motion capture approaches because hands are frequently occluded by a torso on video images during ladder climbing. Thus, the position of cameras is important in minimizing hand occlusions.

1. ABSTRACT.....	1
2. INTRODUCTION	1
2.1 Motivation.....	1
2.2 Specific Aims.....	2
3. TESTING VISION-BASED MOTION CAPTURE.....	3
3.1 Vision-based Motion Capture Systems.....	3
3.2 Multiple Camera-based Approach	4
3.3 Stereo Vision System-based Approach.....	5
3.4 Results and Discussion	6
4. EXTERNAL FORCES DURING LADDER CLIMBING.....	9
4.1 Estimation of External Forces During Ladder Climbing.....	9
4.2 Factors Affecting External Forces During Ladder Climbing	9
4.3 Instrumented Ladder for a Portable Step Ladder.....	10
4.4 Force Prediction Models.....	11
4.5 Results and Discussion	12
5. MOTION DATA-DRIVEN BIOMECHANICAL ANALYSIS	14
5.1 Biomechanical Analysis and Computerized Tools.....	14
5.2 Automated Motion Data Processing for Static Biomechanical Analysis in 3D SSPP™ ...	16
5.3 Automated Motion Data Processing for Dynamic Biomechanical Analysis in OpenSim..	18
5.4 Results and Discussion	21
6. PROTOTYPE OF A FIELD TOOL FOR ON-SITE BIOMECHANICAL ANALYSIS DURING LADDER CLIMBING	22
6.1 Aim of Field Tool	22
6.2 System Architecture.....	23
6.3 System Components.....	24
6.4 Discussion.....	26
7. CONCLUSIONS AND FUTURE RESEARCH	27
7.1 Vision-based Motion Capture.....	27
7.2 External Forces During Ladder Climbing.....	27
7.3 Motion-data Driven Biomechanical Analysis.....	28
7.4 Field Tool for On-Site Biomechanical Analysis.....	28
7.5 Comprehensive Validation.....	28
8. REFERENCES	29
9. APPENDIX.....	32
9.1 User's Manual for the Field Tool.....	32
9.2 Dissemination: Journal Papers and Conference Proceedings	40
9.3 Dissemination: Seminars	41

1. ABSTRACT

Falls from ladders are the leading cause of fatal occupational injuries, and a number of ladder-related injuries have been reported in construction. Lost balance, missed/slipped footing, and lost hand grip, which are common causes of ladder injuries, can result from insufficient force exertion to support the body load on a ladder. Thus, understanding musculoskeletal stresses on the human body during ladder climbing on sites helps to reduce ladder-related injury risks caused by workers' unsafe climbing styles or hazardous ladder conditions. Recently, advancements made in computer vision open the door to collecting workers' motion data without interfering with workers' ongoing work. In this study, we test the feasibility of the computer vision technology in conducting biomechanical analysis during ladder climbing under real conditions. Specifically, we aim to develop a prototype field tool for on-site biomechanical analysis during ladder climbing that monitors and evaluates workers' climbing activities. This field tool also aims to see the feasibility of quantifying the physical demands required to climb a ladder under real conditions. To achieve these aims, the following steps have been made: 1) testing our already-developed vision-based motion capture approaches to collect motion data during ladder climbing; 2) studying external forces exerted on hands and feet and developing a force prediction model to estimate the forces without direct measurement; 3) automating motion data processing for biomechanical analysis in 3D SSPP and OpenSim, which allows the motion data from vision-based motion capture approaches to be seamlessly used for these tools; and 4) developing a prototype of a field tool for on-site biomechanical analysis by combining proposed methods for data collection and data processing procedures. Each step includes case studies to test the feasibility of the proposed methods. The results from case studies showed that the proposed methods and tools have a great potential to be used to estimate musculoskeletal stresses under real conditions. The results also showed that the proposed methods and tools can help us to understand the causes of falls from ladders and potential musculoskeletal injuries during ladder climbing. The findings of this study would be helpful for researchers who are considering adopting new techniques to capture motion data for on-site analysis, as well as for practitioners who would like to see the potential of the advanced vision-based motion capture in practice.

2. INTRODUCTION

2.1 Motivation

Climbing has a high risk of occupational injuries due to the hazardous nature of working from heights (e.g., working at an elevation and being in an unstable posture to coordinate the use of hands and feet). Ladder climbing is an important example. Statistics show that falls from ladders are the leading cause of fatal occupational injuries, accounting for 20% of all fatal falls in 2010 (BLS 2011). Further, the number of ladder-related injuries reported in 2011 was 21,530 in the US (BLS 2012). In addition, due to forceful exertion on hands and feet, the repetitive use of a ladder can cause localized fatigue (Kumar 1999), which may contribute to the development of work-related musculoskeletal disorders in the long term. The National Occupational Research Agenda (NORA), which is a research framework for the U.S. National Institute for Occupational Safety and Health (NIOSH), also considers reducing falls to be among the most critical issues in workplace safety and health, and so set a strategic goal:

- Goal 1.0: Reduce construction workers' fatalities and serious injuries caused by falls to a lower level.

Reducing falls from ladders is a significant part of achieving NORA's Construction Sector Strategic Goal, considering the high frequency of falls from ladders. Common causes of ladder injuries are lost balance, missed/slipped footing, and lost hand grip (Perry and Ronk 2010). From the perspective of ergonomics, all of these causes can be defined as 'insufficient force exertion' in the 'right direction' at the 'right time' to support the 'body load'. In other words, falls from ladders occur when workers are unable to exert sufficient forces to prevent falling (Armstrong et al., 2008). Some studies have described hand and foot forces to identify fall risks during ladder climbing, but few have thoroughly quantified internal forces (e.g., joint moments of human body) induced by motions and external forces as risk factors. This is because of the challenge to evaluate the risk of falls by quantifying the internal forces exerted to support the human body during ladder climbing. Though techniques previously used to prevent falls (e.g., accident investigation, surveys, focus groups, and laboratory experiments) provide valuable insights into fall prevention, these techniques may not be suitable for measuring the physical demands required to climb a ladder under real conditions.

2.2 Specific Aims

To address this issue, the overall aim of this research is to conduct a pilot study that will develop a prototype field-tool to monitor and evaluate worker posture and movement patterns under real conditions from the biomechanics perspective during ladder-climbing activities. Figure 1 shows an overall framework of the proposed field tool. First, we have been developing a technique that extracts the 3D skeletons of workers from video images obtained from cameras, such as ordinary network surveillance cameras mounted on sites. In this study, we will test the technique's accuracy as compared with a subject's ground truth (e.g., bone length). In addition, we explore the feasibility of using portable devices, such as a 3D camcorder and a stereo vision camera, to collect 2D or 3D video images on ladder climbing activities; such images may be difficult to capture using fixed surveillance cameras. The next step is to understand force patterns exerted on hands and feet through laboratory experiments and to model the patterns to predict hand and foot forces during ladder climbing. 3D skeleton-based motion data and predicted force data are combined into static (3D SSPPTM) and dynamic (OpenSim) biomechanical analysis tools to estimate musculoskeletal stresses during ladder climbing activities. The final outcome, a prototype field tool, integrates the processes for data collection and biomechanical analysis, and then provides a visualization of the analysis results or an effective and intuitive interpretation of a particular action or posture taken by a worker during recording and that action's or posture's impact on health and safety during ladder climbing. The feasibility of each research step is examined by conducting experimental case studies. Based on the case studies, findings and challenges encountered are discussed to strengthen the basis for the field tool for on-site biomechanical analysis. Further studies for the proposed field tool are also suggested.

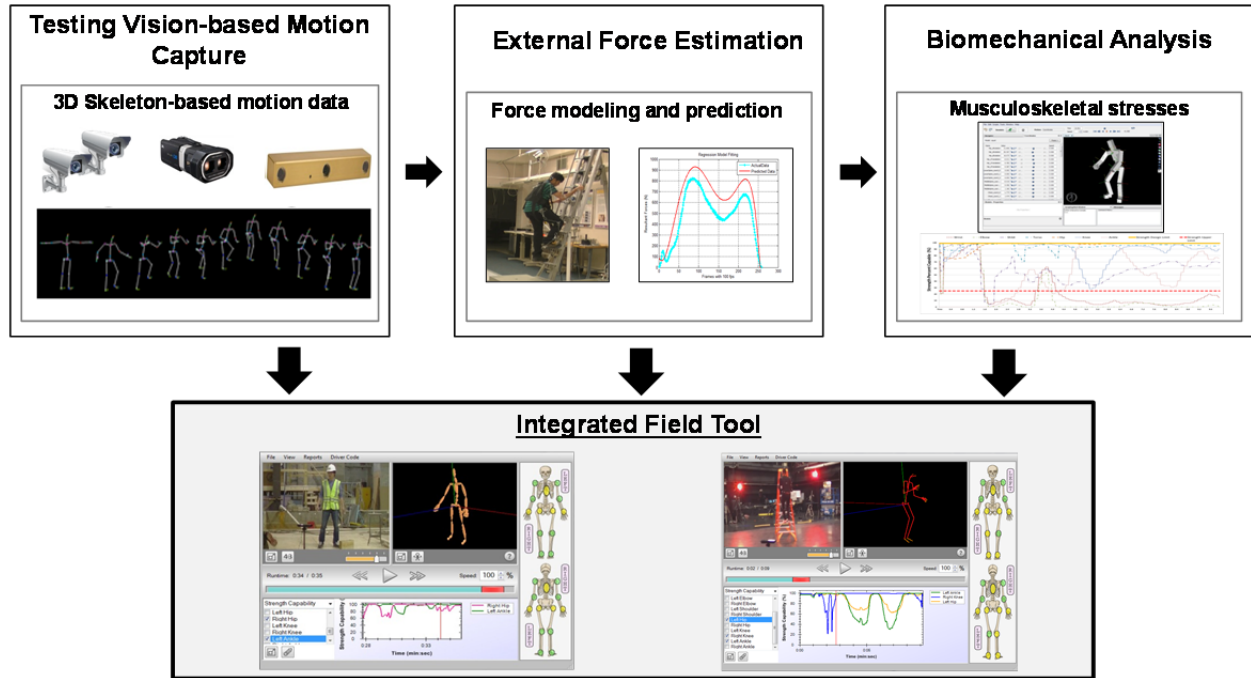


Figure 1. Research overview

3. TESTING VISION-BASED MOTION CAPTURE

3.1 Vision-based Motion Capture Systems

For biomechanical studies on ladder climbing activities, it is essential to collect motion data during the activities. Optical motion capture systems using passive (e.g., retro-reflective) or active markers (e.g., light-emitting diode) attached to a subject's body are the most common techniques for collecting kinematic data for dynamic biomechanical studies (Davis et al. 1991, Aminian and Najafi 2004). However, optical motion capture systems require expensive devices, a controlled environment for lighting conditions, and markers attached to the subject that interfere with on-going works when collecting motion data. Recently, vision-based motion capture approaches have gotten popular because they are the only non-invasive methods for obtaining human motion information (Moeslund et al. 2006). Vast research efforts have developed emerging computer vision techniques or algorithms to extract motion data from video cameras (e.g., 2D images) (Moeslund and Granum 2001, Moeslund et al. 2006, Poppe 2007), and the use of 3D images from RGB-D sensors (e.g., Kinect™) or stereo cameras has simplified the process for vision-based motion capture algorithms (Shotton et al. 2013). The main advantage of the vision-based motion capture is that it does not require any markers or sensors to be attached to the subject during motion capture, and allows researchers to generate human skeleton-based motion data.

In this section, we tested vision-based motion capture algorithms using 2D images from multiple cameras (or a 3D camcorder) and 3D images from a stereo vision camera to collect 3D skeleton-based motion data during ladder climbing. Figure 2 shows a schematic diagram explaining how vision-based motion capture systems work under real conditions. When multiple ordinary network surveillance cameras (at least two cameras required) are placed at the locations of

interest, 2D video images on ladder climbing activities can be obtained and transferred over computer networks to a computer for post-data processing (e.g., vision-based motion capture algorithms). However, due to the continuously changing working environments in construction sites, locations where ladders are used also change depending on construction progress, and thus, there can be a situation where fixed surveillance cameras are difficult to use in capturing ladder climbing activities under real conditions. In this case, portable devices such as a 3D camcorder or a stereo vision camera can be used to collect video images. We have investigated a potential use of the aforementioned vision-based motion capture approaches as a field-based motion measurement method for ladder climbing activities.

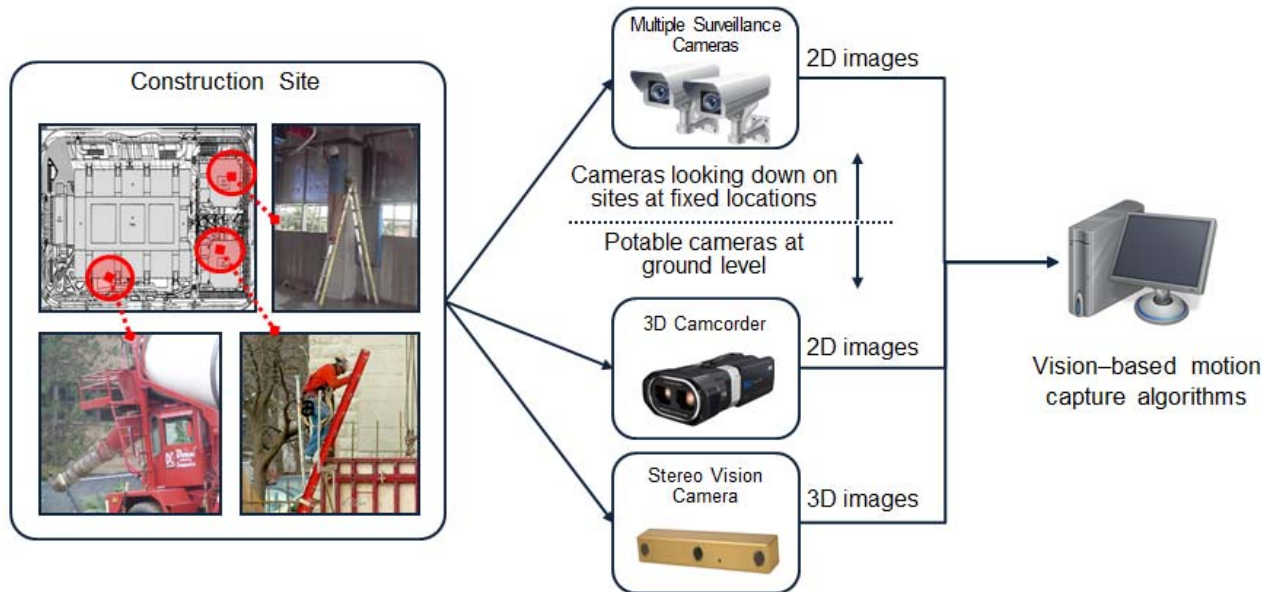


Figure 2. Schematic diagram of vision-based motion capture

3.2 Multiple Camera-based Approach

One of the vision-based motion capture approaches we tested is the multiple camera-based motion capture approach (Han and Lee 2013). The multiple camera-based motion capture approach uses at least two cameras with different viewpoints or a 3D camcorder. When multiple ordinary surveillance cameras are used, videos from different cameras need to be synchronized before data processing on video images. On the other hand, a 3D camcorder is composed of two lenses in one camera, thus producing two synchronized videos from different viewpoints. The use of a 3D camcorder allows for the simplification of 3D skeleton extraction to 2D pose estimation while still having the merit of using one device for motion. Vision-based motion capture algorithms using multiple cameras consist of four sequential steps: 1) collection of 2D images using multiple cameras (Figure 3A), 2) 2D pose estimation from one image (Figure 3B), 3) correspondence matching (Figure 3C), and 4) depth computation (Figure 3D) (Han and Lee 2013).

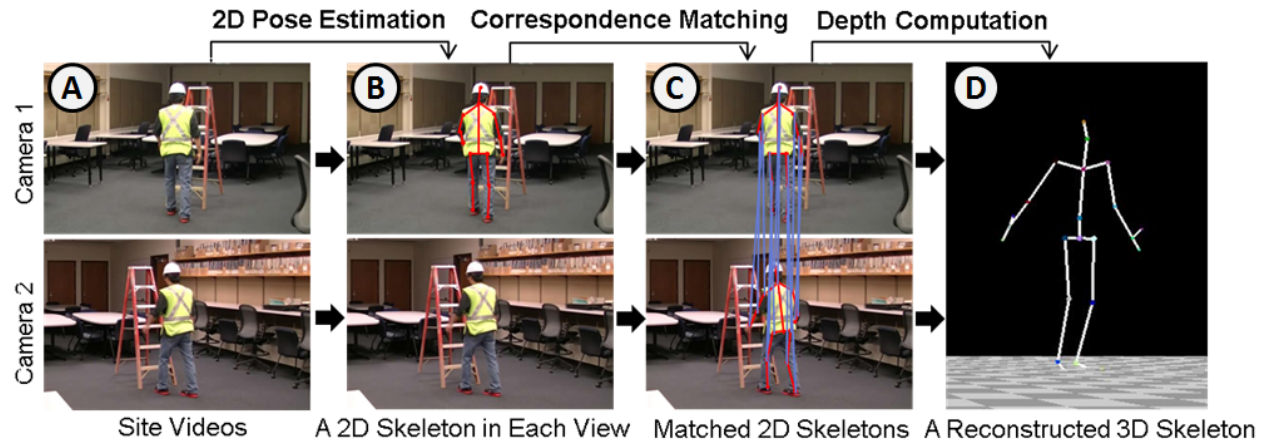


Figure 3. Pipeline for vision-based motion capture using multiple cameras (Han and Lee 2013)

The first step for the multiple camera-based motion capture method is 2D pose estimation, which is the process used to extract a 2D skeleton using the video images from one camera. 2D pose estimation has been based on the articulated pose estimation algorithm with flexible mixtures-of-parts (Yang and Ramanan 2011), which estimates the location of body joints on 2D images. Then, the 2D skeleton is inferred based on the detected body joints.

Given 2D pose estimation results from one image, the correspondence matching process finds corresponding body joints on images from the other view. To determine pixel correspondence on two-view images, we applied a feature-based approach that detects the features of a pixel with feature descriptors (e.g., SIFT (Liu et al. 2011), SURF (Uijlings et al. 2010)), and finds conjugate pairs by comparing the extracted features from images with different viewpoints. Then, the conjugate pairs are used to compute a fundamental matrix that determines corresponding body joints from the image from the other view. In addition, we applied the homography computed from the normalized Direct Linear Transformation (DLT) algorithm (Hartley and Zisserman 2000) to find the potential regions of corresponding points.

As a final step, using the pairs of corresponding body joints from two images with different viewpoints and projection matrices of two cameras, the 3D positions of each body joint are computed through triangulation. A straightforward means to computing the camera projection matrix is to record a chessboard with each camera and obtain camera parameters using available camera calibration toolboxes (e.g., Robust Automatic Detection Of Calibration Chessboards toolbox (Kassir and Peynot 2010)).

3.3 Stereo Vision System-based Approach

We also applied stereo vision system-based approach that extracts 3D skeletons directly from 3D images obtained from a stereo vision camera. With the advent of RGB-D sensors, the use of 3D images for motion capture is getting popular because it doesn't require sophisticated camera calibration and 3D reconstruction processes (Shotton et al. 2013). One of the commonly used devices to collect 3D images is an infrared-based RGB-D sensor (e.g., KinectTM). There is a commercially available motion capture solution using a KinectTM, such as iPi Desktop Motion Capture (www.ipisoft.com), and thus users can easily obtain 3D skeleton-based motion data. However, the infrared RGB-D sensor is severely impeded by sunlight and ferromagnetic radiations and has a limited operating range (Weerasinghe et al. 2012). To address this issue, we

investigated the use of a stereo vision camera system to collect 3D images (Starbuck et al. 2014). The stereo vision camera used in this project is a Bumblebee XB3™ manufactured by Point Grey Technologies (ww2.ptgrey.com). Multiple camera lenses equipped in one device capture a scene from different positions, and correspondence algorithms determine the distance disparity between pixels in each of the two images. The result is a disparity map (i.e., 3D images) from which real-world depth can be computed for any point within the camera’s field-of-view. The advantage of using a stereo vision camera system is that it allows for both optical and depth data to be collected with few environmental restrictions (e.g., outdoor environments) and a limited field-of-view.

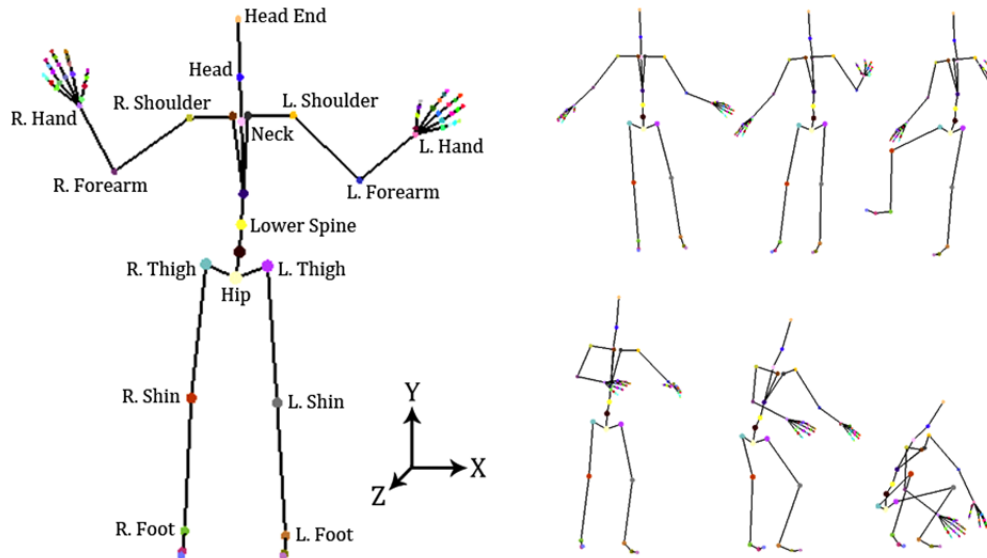


Figure 4. Skeleton-based motion data in BVH file format (Starbuck et al. 2014)

The data collected from the stereo camera are converted into a format used by an existing kinematic modeling software solution—iPi Desktop Motion Capture solution—that is designed for use with a Kinect™. 3D skeleton-based motion data is extracted using the iPi Desktop Motion Capture solutions by replacing 3D images from a Kinect™ with converted 3D images from a stereo vision camera system. The software uses these data to perform skeletal tracking and the results are outputted into a standard motion capture file format, as shown in Figure 4.

3.4 Results and Discussion

To test our vision-based motion capture approach, we conducted experimental case studies. For the multiple camera-based approach, one male subject (height: 175 cm, weight: 75 kg) was asked to repeatedly ascend and descend a portable step ladder using his own climbing style. During the climbing, 5625 frames of videos (about 190 seconds) from a 3D camcorder were collected and processed to extract 3D skeletons representing motions. The resulting 3D skeletons were validated based on the length of body joints (i.e., bone length) by comparing the skeletons with the anthropometry data directly measured from the subject. In Table 1, means and standard deviations of 13 bones’ sizes from 3D skeletons are computed during the trial, and the differences from the anthropometry data are presented. In total, the average difference in bone size in a 3D coordinate is 6.3 cm between the two datasets; taking into account that the difference is derived from the combined results of both 2D pose estimation and 3D

reconstruction, the result shows that, overall, no significant errors arise in either process. However, the differences of right and left arms associated with hands are relatively large, and this suggests that hands may be the most difficult body part to capture with a video. In addition, the inaccuracy could be caused by self-occlusions (i.e., a left arm and hand are occluded by one’s torso in most frames).

Table 1. Bone length comparison of extracted 3D skeletons and the subject’s anthropometry data (Han and Lee 2013)

Bone	Pelvis	Left up-leg	Left leg	Right up-leg	Right leg	Spine	Neck	Left shoulder	Left fore-arm	Left arm	Right shoulder	Right fore-arm	Right arm
Anthropometry (cm)	27	44	43	44	43	61	20	22	36	30	22	36	30
Skeleton Mean/Std. (cm)	24.0 /9.7	38.1 /10.7	39.4 /2.1	37.7 /9.5	32.9 /1.2	70.1 /5.3	22.4 /1.8	33.2 /6.0	24.6 /6.2	24.3 /13.0	22.0 /3.1	26.3 /3.8	22.3 /9.3
Diff. (cm)	-3.0	-5.9	-3.6	-6.3	-10.1	8.1	1.4	10.2	-10.4	-5.7	-1.0	-8.7	-7.7

To test the stereo vision system–based approach, a controlled experiment was performed. Han et al. (2012) have studied the accuracy of motion data by collecting and comparing motion data from the RGB-D sensor–based motion capture system and the optical motion capture system (VICON™), and have found that the RGB-D sensor–based approach showed about 10 degrees of error in body angles. In this study, we compared joint positions in 3D skeleton–based motion data extracted from the stereo vision system–based approach with those from the existing RGB-D sensor–based motion capture system. One male subject (height: 185 cm, weight: 85 kg) was asked to perform basic tasks—such as walking, sitting, and standing—for about 20 seconds, and 3D images were simultaneously captured using a Microsoft Kinect™ and a stereo vision camera during the tasks. Then, the 3D images were processed to extract motion data in the BVH file format using iPi motion capture solutions, as shown in Figure 5.

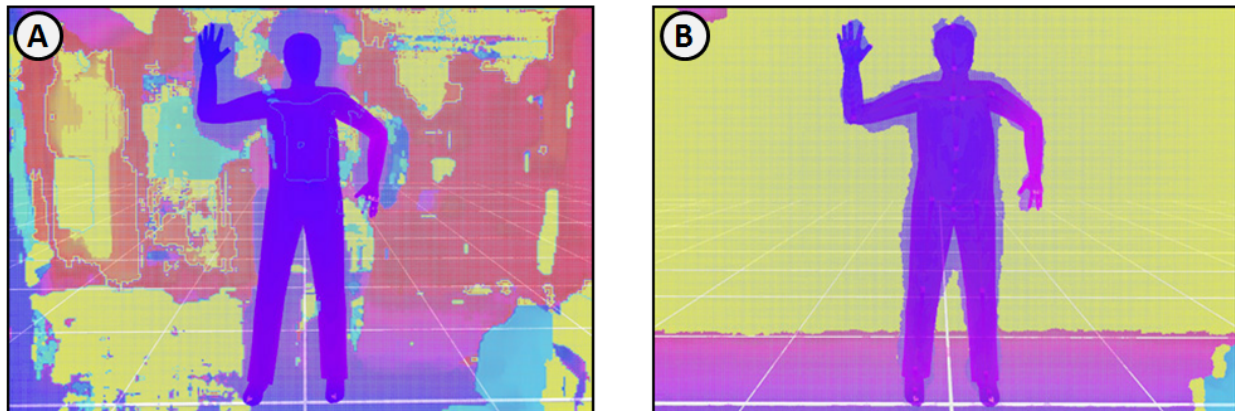


Figure 5. Pose estimation from 3D images in iPi motion capture solutions. A: 3D image from a Microsoft Kinect™. B: 3D image from a stereo vision camera system. (Starbuck et al. 2014)

For each of the BVH motion capture files, the 3D positions of the joints of interest were computed using a transformation matrix from translation and rotation data contained in the files. The computed joint locations from each method were evaluated using the mean absolute error (MAE) in the X, Y, and Z dimensions. Additionally, the magnitudes of those errors were computed for each joint. As shown in Table 2, the mean absolute error in position averaged over all of the joints of interest was 6.826 cm. Similar to the results from the camera-based approach, hands and feet produced the largest errors.

Table 2. Mean absolute errors of estimated joint positions (cm) recorded by Microsoft Kinect™ and Bumblebee XB3™ in a controlled experiment (Starbuck et al. 2014)

Joint Name	MAE _x	MAE _y	MAE _z	MAE
Hip	3.2 cm	4.7 cm	1.4 cm	5.9 cm
Lower Spine	2.7 cm	4.6 cm	2.7 cm	6.0 cm
Neck	2.9 cm	4.3 cm	4.7 cm	7.0 cm
Head	3.0 cm	4.2 cm	2.7 cm	5.8 cm
Head End	3.6 cm	4.4 cm	1.7 cm	6.0 cm
L. Shoulder	2.9 cm	3.8 cm	4.7 cm	6.7 cm
R. Shoulder	3.4 cm	4.0 cm	5.2 cm	7.4 cm
L. Forearm	3.6 cm	3.0 cm	3.6 cm	5.9 cm
R. Forearm	3.2 cm	3.4 cm	3.3 cm	5.8 cm
L. Hand	4.8 cm	3.9 cm	5.6 cm	8.4 cm
R. Hand	5.3 cm	5.5 cm	6.3 cm	10.0 cm
L. Thigh	2.8 cm	5.1 cm	2.3 cm	6.3 cm
R. Thigh	3.3 cm	4.4 cm	3.0 cm	6.2 cm
L. Shin	2.2 cm	5.3 cm	2.4 cm	6.2 cm
R. Shin	3.1 cm	5.1 cm	1.2 cm	6.1 cm
L. Foot	1.2 cm	5.7 cm	3.9 cm	7.0 cm
R. Foot	3.7 cm	4.9 cm	7.5 cm	9.7 cm
Mean	3.2 cm	4.5 cm	3.7 cm	6.9 cm

Though 3D skeletons have been extracted from multiple camera and stereo vision camera-based motion capture approaches with reasonable accuracy, challenging issues remain when we apply these approaches to real-world situations, such as ladder climbing activities, and when we aim to improve the accuracy. Both approaches had difficulty tracking hand positions due to self-occlusion. To avoid self-occlusions, the locations of cameras with clear viewpoints on workers would be critical. For example, even though a 3D camcorder or a stereo vision camera captures images with two camera lenses, the viewpoints from the lenses are almost the same, resulting in a higher possibility of occlusions than with the use of multiple cameras that have completely different viewpoints. In addition, the short distance between lenses in a 3D camcorder and a stereo vision system may result in poor performance regarding the capture of accurate depth information through triangulation algorithms. Therefore, despite the advantage of using a single 3D camcorder or stereo vision camera, using multiple cameras with different viewpoints, or

using two stereo vision cameras, may alleviate accuracy issues due to occlusions or a short distance between lenses.

4. EXTERNAL FORCES DURING LADDER CLIMBING

4.1 Estimation of External Forces During Ladder Climbing

External forces are gravity, friction, and impact with the floor and other external objects that are applied to the body (Chapman 2008). These external forces combined with postural requirements produce internal forces as a result of muscle action. Therefore, for biomechanical analysis during ladder climbing activities, external forces should be obtained along with motion data.

During ladder climbing, external forces can be described by measuring hand and foot forces. Foot forces are the ground reaction forces pushing against the foot, and hand forces are the forces required to grip a rung or a rail. Though direct measurement (e.g., load cells) of forces in the laboratory that has been used previously provide valuable insight into external forces during ladder climbing, it is very difficult to measure those forces directly on a ladder in real construction sites. Taking into consideration real conditions in ladder climbing in construction, we need to predict external forces based on available data, so that biomechanical analysis will be enabled.

Several research efforts conducted in the laboratory showed that hand and foot forces are strongly linked with climbing behaviors or styles. For example, Armstrong et al. (2008) found that the average hand force is 42.4% of bodyweight in rung climbing, and 32.2% of bodyweight in rail climbing. According to Bloswick and Chaffin (1990), the resultant hand force decreased from 25% to 10% of a total body load as the inclination of the ladder changed from 90° (vertical) to 70°. Häkkinen et al. (1988) carried out laboratory studies to survey the loads during ladder climbing, concluding that individual climbing styles seem to affect the forces and displacements of a ladder. From these research efforts, we hypothesized that force patterns (i.e., profiles) might be similar under the same climbing styles with the same ladder conditions. In other words, force profiles that are collected from laboratory experiments under various climbing styles or ladder conditions can be used to predict forces under the same conditions.

To estimate external forces during ladder climbing without direct measurement, we explored experimental force data-driven prediction. Before collecting force data during ladder climbing through experiments, we identified dominant factors affecting external forces during ladder climbing from literature. Then, to test the feasibility of the proposed experimental force data-driven prediction, we designed a laboratory experiment for ladder climbing on a portable step ladder, and collected hand and foot forces. The data collected from experiments was modeled to predict external forces during ladder climbing with the same factors under real conditions.

4.2 Factors Affecting External Forces During Ladder Climbing

There have been several research efforts to identify the relationships between average/peak hand and foot forces and factors during ladder climbing. For example, Bloswick and Chaffin (1990) conducted extensive experiments to identify statistical relationships between various independent factors (e.g., rung separation, ladder slant, climbing speed and direction, climbing style, and anthropometry) and average hand and foot forces, and found that ladder slant and climbing style

were key factors explaining the variations in the average forces. From the study on peak forces on feet during ladder climbing, Lee et al. (1994) found that a higher ladder slant resulted in a greater posterior displacement of the center of the body, which increased foot forces. In addition, even in the same ladder slant, such as a vertical ladder, hand forces ranged from 20% to 36% of the total body weight according to subjects' climbing styles (Ayoub and Bakken 1978). Based on the literature review on these previous research efforts, we classified different factors that have been known to affect forces into individual and task factors, as shown in Table 3.

Table 3. Force-related factors from literature

Factors		Variables
Individual factors	Physical components	Height (e.g., short/average/tall) (Bloswich and Chaffin 1990)
		Weight (e.g., light/average/heavy) (Bloswich and Chaffin 1990)
	Preference components	Gait style (e.g., lateral/diagonal, two beat/four beat) (McIntyre 1981, Armstrong et al. 2008)
		Body posture (e.g., position of the body's center of mass from a ladder, hand-foot distance) (Bloswich and Chaffin 1990, Armstrong et al. 2008)
	Climbing velocity (Armstrong et al. 2008)	
Task factors	Physical components	Rung separation (Bloswich and Chaffin 1990, Häkkinen et al. 1988)
		Ladder slant (Bloswich and Chaffin 1990, Armstrong et al. 2008)
		Rung shape (e.g., round and rectangular rungs, steps) (Häkkinen et al. 1988)
	Action components	Climbing direction (e.g., ascending/descending) (Bloswich and Chaffin 1990, Armstrong et al. 2008)
		Load carriage (e.g., tool box, hand tool) (Armstrong et al. 2008)

4.3 Instrumented Ladder for a Portable Step Ladder

To measure hand and foot forces during ladder climbing for a portable step ladder—the most common type of ladder used in construction sites—an instrumented ladder has been constructed, as shown in Figure 6. The configurations of the instrumented ladder reflect the ones of a portable step ladder. According to the Safety and Health Regulations for Construction (Standard Number: 1926.1053(a)) provided by the Occupational Safety & Health Administration (OSHA), steps shall be spaced not less than 10 inches (25 cm) apart, or more than 14 inches (36 cm) apart. The minimum clear distance between the side rails for all portable ladders shall be 11 1/2 inches (29 cm). In addition, a non-self-supporting ladder should have a set-up angle of about 75 degrees. Considering the standards, a vertically tilted ladder (75 degrees) with 12 inches (30 cm) of step spacing, and 16 inches of distance between the side rails was designed. The rungs and rails were mounted on 3-axis force and 3-axis moment transducers. The outputs from the transducers are combined electronically to provide resultant x, y, and z forces on the rails. Software provided with each system is used for the acquisition and to synchronize the measurements.

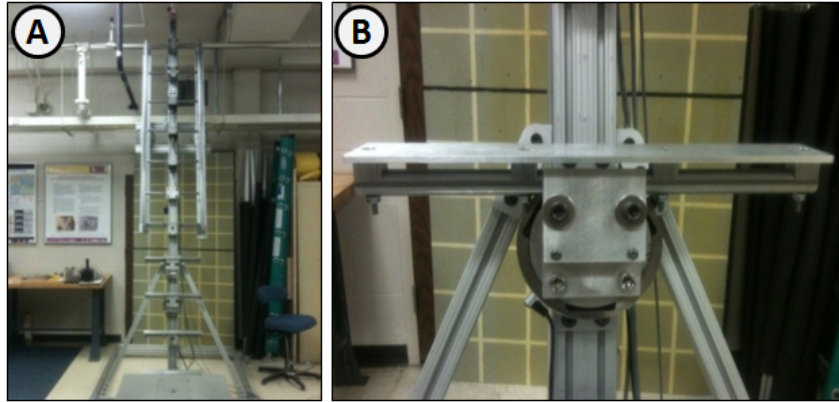


Figure 6. Instrumented ladder. A: Front view. B: A step and a load cell. (Seo et al. 2014a)

4.4 Force Prediction Models

The previous study conducted by Armstrong et al. (2008) found that force patterns during ladder climbing showed three phases according to force exerting timing: inclining phase, stabilizing phase, and declining phase. To model these distinctive patterns, we applied two different models; one is a linear model, and the other is a polynomial regression model.

Figure 7 shows configurations of a linear model. For example, the model is designed to reflect peak forces during the inclining phase and declining phase by using parameters, $F_{\text{peak},a}$ and $F_{\text{peak},b}$. We also assume that the force represented by F_{stable} is constant during the stabilizing period (Period b in Figure 7). To obtain the model that fits observed force data well, we applied a genetic algorithm–based fitting method to minimize the average of the Normalized Root Mean Square Errors (NRMSEs) between the proposed force profiles and measured force profiles in each time frame.

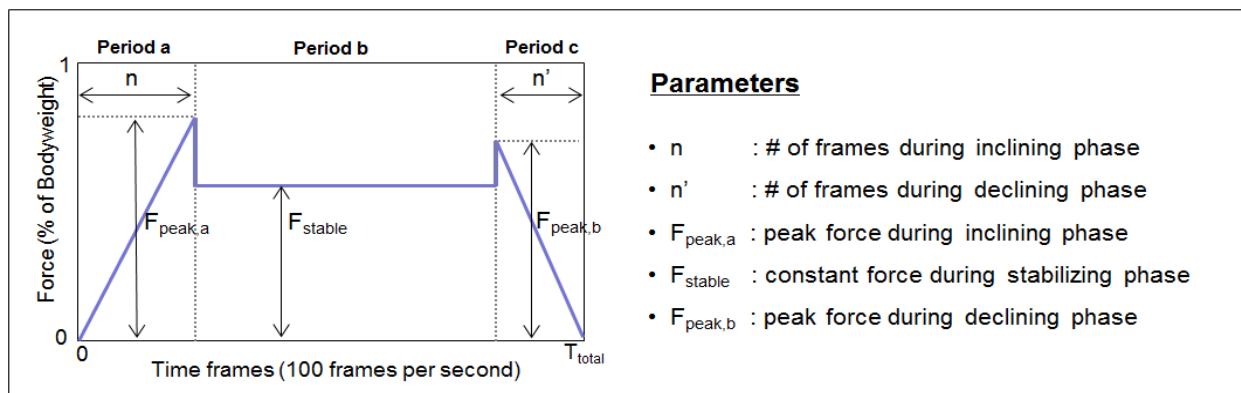


Figure 7. Force model fitted to observed hand and foot forces (Seo et al. 2014a)

Also, a polynomial regression model was applied to model the relationship between the independent variable x (time frames) and the dependent variable y (resultant hand and foot forces) as an n -th order polynomial. The model was fitted to observed force data by using the method of least squares. In addition, the optimum order of a polynomial was determined to have the least sum of the squares of the residuals.

4.5 Results and Discussion

To test the feasibility of the proposed models for prediction, we collected force profiles using the instrumented ladder under specific conditions. To collect force data under identical conditions, two male subjects who had similar weights (Subject #1: 73 inches/180 lbs, Subject #2: 67 inches/176 lbs) were recruited from the University community. In addition, the subjects were asked to ascend and descend the same ladder repeatedly using a diagonal gait at a high speed. Hand and foot forces were collected from the force transducers mounted on the ladder at 110 Hz. The total resultant force profiles (magnitude of forces) from Subject #1 were used to fit the linear and polynomial models. The models were fitted to hand and foot forces during ascending and descending, respectively.

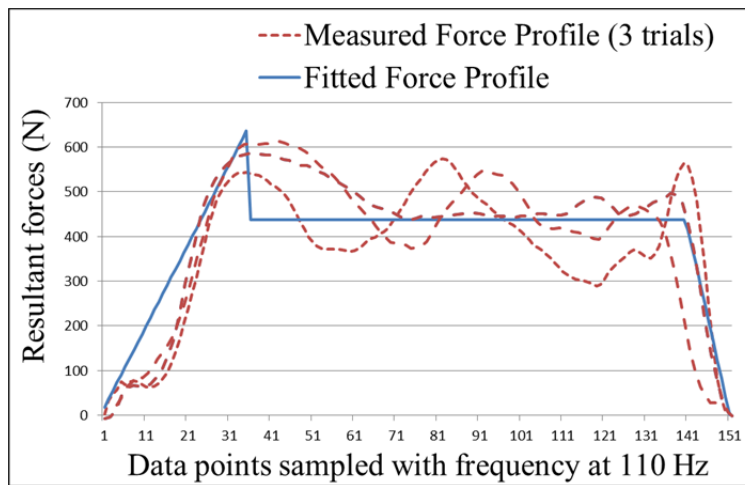


Figure 8. An example of a fitted linear model (Seo et al. 2014a)

Figure 8 shows an example of a fitted linear model for foot forces of three trials during ascending, and Table 4 shows fitted values for each of five parameters of the linear models. The n values during ascending are higher than during descending, which means that the body weight is transferred to rails and rungs faster when a subject descends a ladder.

Table 4. Parameters in force prediction models (Seo et al. 2014a)

Body Parts	Ascending					Descending				
	n (#of frames)	n' (#of frames)	F _{peak,a} (% of BW)	F _{stable} (% of BW)	F _{peak,b} (% of BW)	n (#of frames)	n' (#of frames)	F _{peak,a} (% of BW)	F _{stable} (% of BW)	F _{peak,b} (% of BW)
Right Hand	105	62	0.25	0.13	0.22	44	41	0.13	0.13	0.14
Left Hand	157	62	0.33	0.14	0.27	56	40	0.15	0.13	0.11
Right Foot	119	52	1.38	0.93	1.18	52	110	0.96	0.95	1.28
Left Foot	104	27	1.47	0.97	1.00	57	107	1.01	1.00	1.28

Figure 9 shows polynomial regression models fitted to observed force data from Subject #1. Azure lines indicate force data obtained from Subject #1 while red lines mean fitted regression models.

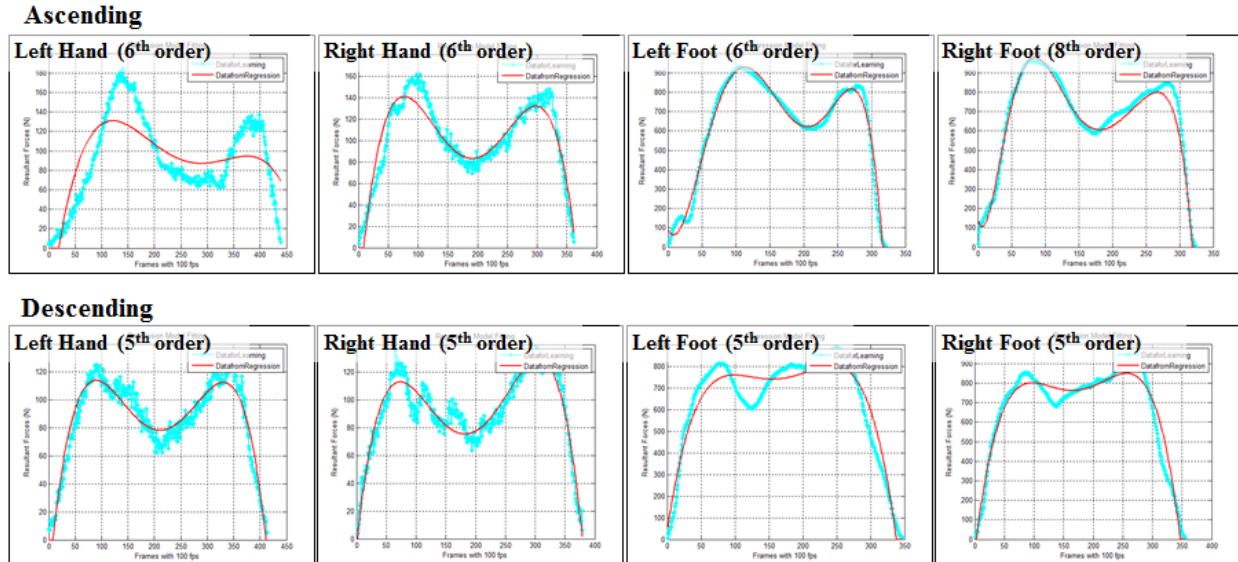


Figure 9. Polynomial regression models fitted to data

Using linear and polynomial regression models, the magnitudes of hand and foot forces were predicted for Subject #2, and were compared with measured values (Table 5). The values of the Normalized Root Mean Square Error (NRMSE: RMS divided by mean value) between predicted foot forces and measured foot forces on each time frame were 0.424 for hand forces and 0.292 for foot forces from linear models; and 0.295 for hand forces and 0.159 for foot forces from polynomial regression models. In addition, polynomial regression models predict peak forces more accurately than linear models. These results indicate that polynomial regression models captured overall force patterns well, and thus show better prediction performance than linear models. However, even though polynomial regression models provided relatively better prediction in terms of NRMSE and peak forces, the average forces were well captured by the linear models, showing an error of about 10%. Because the linear model was intended to fit force data using a few polylines, it is difficult to capture dynamic patterns in force profiles. However, the linear model captured force patterns during the stabilizing period better than the polynomial regression model, and thus provided more accurate prediction results for average forces.

Table 5. Validation of force prediction models

Models	Body Part	Force Prediction		
		NRMSE	Peak Force (% error)	Average Force (% error)
Linear	Hand	0.424	15.7%	9.9%
	Foot	0.292	19.4%	11.9%
Polynomial regression	Hand	0.295	12.7%	18.2%
	Foot	0.159	8.0%	20.0%

Even though the prediction performance varied depending on the types of models for data fitting, the results from the test showed that the experimental data-based force prediction has a great potential to obtain external force data during ladder climbing without direct measurement. However, we tested the proposed method only in certain conditions (e.g., portable step ladder,

diagonal climbing). For future research, extensive experiments to collect hand and foot forces need to be further conducted by varying factors affecting forces during ladder climbing. Then, force models under dominant factors need to be examined to validate the proposed method under diverse conditions. In addition, different fitting methods may perform better to explain unique patterns in force profiles, and thus increase estimation accuracy.

5. MOTION DATA-DRIVEN BIOMECHANICAL ANALYSIS

5.1 Biomechanical Analysis and Computerized Tools

Biomechanical models describing complex musculoskeletal systems of the human body help to estimate internal forces that can rarely be measured directly (Chaffin et al. 1996). Based on the assumption that the actions of the human body follow the laws of Newtonian mechanics, the biomechanical models provide a quantitative assessment of the musculoskeletal loads (e.g., joint moments) during occupational tasks, which helps one to identify hazardous loading conditions on certain body parts (Radwin et al. 2001).

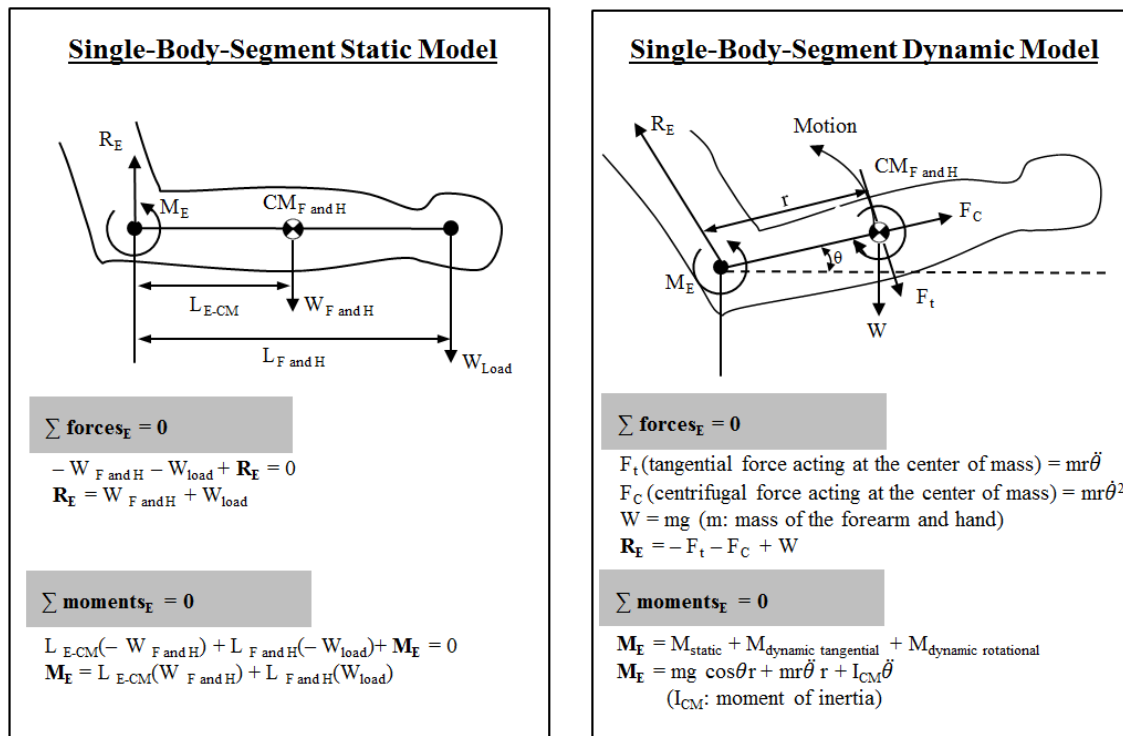


Figure 10. Comparison between static and dynamic biomechanical models (Chaffin et al. 2006)

Various biomechanical models have been developed, and they are classified into static and dynamic models according to whether or not the models consider inertial forces that are produced by changes in the velocity and direction of the motion (Chaffin et al. 2006). Figure 10 illustrates the differences between static and dynamic biomechanical models based on a single body segment (i.e., forearm and hand) (Chaffin et al. 2006). The underlying assumption for biomechanical models is that the sum of reactive forces and moments at each body joint is zero in both static and dynamic conditions (i.e., static and dynamic equilibrium). In the single-body-

segment models, it is also assumed that the forces act in a single plane. While the static model determines the reactive force and moment at the elbow based on anthropometric, postural, and external load information, the dynamic model considers additional inertial forces such as tangential or centrifugal forces for reactive forces, and instantaneous ($M_{\text{dynamic tangential}}$) and rotational ($M_{\text{dynamic rotational}}$) acceleration effects on joint moments due to dynamic motions.

The resulting values that are obtained by solving the equilibrium equations for the load moments and reactive forces at the joint (e.g., elbow) adjacent to the application of an external load (e.g., hand loads) will be used to solve the equilibrium conditions for the next adjacent joint (e.g., shoulder). By repeating these procedures for connective body joints in the kinetic linkage system, all joint moments and external reactive forces can be obtained. For the comprehensive evaluation of many occupational tasks, three-dimensional analysis of joint moments and reactive forces is required using six independent equilibrium equations with respect to three orthogonal axes at each joint ($\sum F_x=0$, $\sum F_y=0$, $\sum F_z=0$ for reactive forces; and $\sum M_x=0$, $\sum M_y=0$, $\sum M_z=0$ for joint moments). Because an estimation of internal loads requires tedious computations with three-dimensional whole-body biomechanical models, several computerized software packages for static biomechanical analysis (e.g., 3D SSPPTM (Three-Dimensional Static Strength Prediction ProgramTM)) and dynamic biomechanical analysis (e.g., OpenSim, Visual 3-DTM, and AnyBodyTM) have provided practical solutions to study musculoskeletal stresses.

However, the skeleton-based motion data obtained from vision-based approaches in Section 3 are not readily applicable to existing biomechanical analysis tools. For example, 3D SSPPTM (Chaffin et al. 2006)—the only available computerized static biomechanical analysis tool designed to evaluate static postures or motions without acceleration—defines a human posture with horizontal and vertical angles in a global coordinate system (i.e., defined for a full body). OpenSim (Delp et al. 2007)—one of the popular dynamic analysis tools that considers inertial forces caused by acceleration—simulates motions using marker-based motion data that contains the positions of markers rather than body joints (i.e., more than one marker is generally attached to one body joint). Nevertheless, vision-based motion capture systems generally characterize motions using Euler rotation angles at a body joint in a local coordinate system (i.e., defined for each body joint), for example, as in the Biovision Hierarchical (BVH) format (Meredith and Maddock 2001). In this regard, a motion data reconfiguration that converts motion capture data into the proper form for ergonomic analysis tools is the key to the successful implementation of on-site biomechanical analysis.

In this section, we propose a motion data–driven biomechanical analysis on construction manual tasks using motion data obtained from vision-based motion capture approaches. Specifically, we semi-automate the process to convert the motion data into available data and represent motions in biomechanical analysis tools (Seo et al. 2014b). As biomechanical analysis tools to be studied, 3D SSPPTM and OpenSim are selected because they are not only widely used static and dynamic biomechanical analysis tools, but because they also enable us to customize existing functionality to run biomechanical analysis.

5.2 Automated Motion Data Processing for Static Biomechanical Analysis in 3D SSPPTM

3D SSPPTM is static biomechanical analysis software developed by the Center of Ergonomics at the University of Michigan (Chaffin et al. 2006). With posture data, anthropometry data, and force parameters, workers' motions can be simulated in a virtual 3D environment. Based on the biomechanical simulation, static strength requirements (e.g., joint moments) for certain tasks are

predicted. This includes the spinal compression force using the static biomechanical model (Center for Ergonomics, University of Michigan 2011) that assumes the effects of acceleration and momentum are negligible. Importantly, based on the analysis results of postures, the body parts that endure forceful exertion can be found as compared with the relevant human capacity (NIOSH 1981). Figure 11A shows an example of the biomechanical analysis result in 3D SSPP. The left three images in Figure 11A are the same pose from different viewpoints, and the right image in Figure 11A shows the analysis result. The limits in the bar graphs—green to yellow transition, and yellow to red transition—correspond to the NIOSH Action Limit and Maximum Permissible Limit, respectively (NIOSH 1981). If the bar that represents joint moments in this pose is in the red zone, the body segment has a high risk of getting injured.

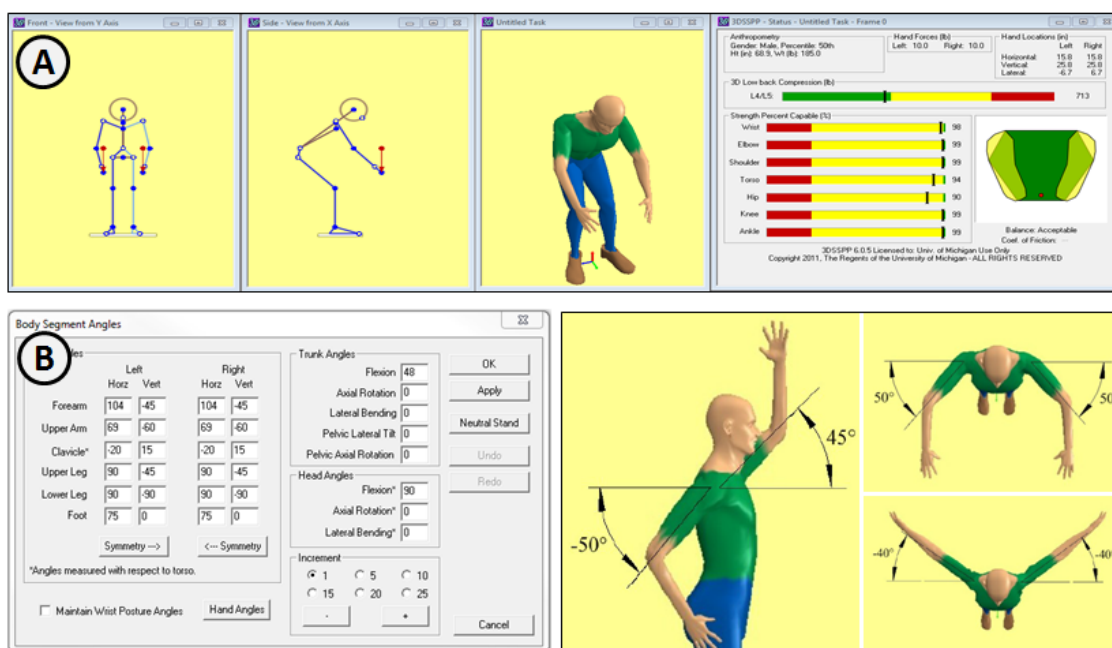


Figure 11. 3D SSPP™. A: User interface. B: Angular configurations of a human model.

In 3D SSPP™, anthropometric factors such as height and weight are used to adjust the body lengths, masses, and centers of mass of body segments in the biomechanical body model. Force parameters referring to hand forces during lifting, pushing, and pulling—foot forces are determined by a sum of body weight and hand force vectors—specify external forces during tasks. While anthropometric factors and force parameters can be included by simply inputting them in 3D SSPP™, postural angles should be determined from motion data. Postures of the body model can be defined as body segment angles, specifying about 41 angles for the body (horizontal and vertical angles for each body part) and inputting them in each frame, as shown in Figure 11B.

While postures in 3D SSPP™ are defined as the horizontal and vertical angles of body parts, the BVH motion data defines the hierarchical and spatial structure of a human body and stores 3D rotation angles and a 3D position of a root body joint (e.g., a hip) at each frame. To compute the horizontal and vertical angles required for 3D SSPP™, first, 3D positions (x-y-z coordinates) of all of the body joints are iteratively computed from the root joint using translations and rotations (i.e., a transformation matrix), based on the predefined hierarchical structure of a body. Then, the

joint angles are computed based on the vectors of bones between two connected body joints in a local coordinate system of the body, following the definitions of horizontal and vertical angles for each body joint in 3D SSPP™ (Center for Ergonomics, University of Michigan 2011). For example, the vertical and horizontal angles of upper arms for 3D SSPP™ (See Figure 12A) were calculated from two vectors—a vector from a neck joint to a shoulder joint, and a vector from a shoulder joint to an elbow joint (See Figure 12B).

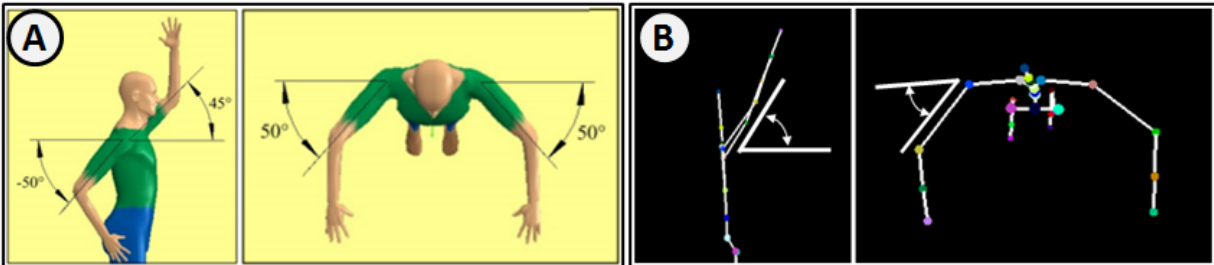


Figure 12. Vertical and horizontal angle of upper arm. A: in 3D SSPP™. B: in the BVH motion data.

The postural angles calculated from the BVH motion data for each frame are integrated in a batch file that allows for the automatic analysis of tasks just by importing the batch file into 3D SSPP™ (Center for Ergonomics, University of Michigan 2011). Figure 13A show an example of a batch file automatically generated, containing information to run a biomechanical analysis in 3D SSPP™. All lines in the batch file have one command describing relevant data. Types and functions of commands used in a batch file are illustrated in Figure 13B. In addition, the results (e.g., summary results, joint moments, strength capabilities, etc.) from a biomechanical analysis in 3D SSPP™ can be exported as an external text file (.exp) for further analysis.

A Example of batch file

```

3DSSPPBATCHFILE #
COM #
DES 0 "Example of Batch File" #
AUT 1 #
ANT 0 3 68.9 185 #
FRM 1 #
JOA 16.9698 -7.57020 16.9698 -7.5702 12.2084
-10.7369 -20 0 -0.64244 -64.0564 -88.9659
-85.4295 85.136 -5.7582 2.2298 -4.3079 0 2.2298
-4.3079 0.85105 -4.8446 -2 0 0 -23.9018
-80.3754 -28.722 -81.1688 93.9952 -7.998 88.3453
0 -4.0454 0 0 0 78.44 -2.2991 1.3629
0 0 #
HAN 20 -90 0 20 -90 0 #
EXP #
AUT 1 #
FRM 2 #
JOA 18.0219 -7.95020 18.0219 -7.9502 12.6864
-11.2829 -20 0 0.90062 -63.8582 -86.4393
-84.6193 87.5135 -5.9056 2.0483 -4.08140 2.0483
-4.0814 -0.30886 -4.8004 -20 0 -23.6184
-80.5151 -28.331 -81.3217 94.208 -8.3682 87.8099
0 -3.7762 0 0 0 78.6671 -2.18 1.2585
0 0 #
HAN 20 -90 0 20 -90 0 #
EXP #
AUT 1 #
                    
```

B Commands in batch file

- First line
 - must be 3DSSPPBATCHFILE #
- COMMENT command
 - COM Anything you want to type to document your file. #
- DESCRIPTION command
 - DES 0 (English unit) or 1 (Metric unit) "Task Name" #
- AUTOEXPORT command
 - AUT 0 (Do not export the results) or 1 (Export the results) #
- ANTHROPOMETRY Command
 - ANT 0 (Male) or 1 (Female) 3 (set according to the next two data) Height Weight #
- FRAME Command
 - FRM Frame numbers. #
- SEGMENTANGLES Command
 - JOA 41 body segment angles (e.g., Hand left horizontal, hand left vertical, hand left rotation, forearm left horizontal....) #
- HANDLOADS Command
 - HAN Left magnitude, left vertical angle, left horizontal angle, right magnitude, right vertical angle, right horizontal angle #
- EXPORT Command
 - EXP (no data item, just for initiating data exports) #

Figure 13. Batch file to run 3D SSPP™. A: Example of a batch file. B: Commands in a batch file. (Seo et al. 2014b)

5.3 Automated Motion Data Processing for Dynamic Biomechanical Analysis in OpenSim

OpenSim (Delp et al., 2007) is a freely available software package that estimates biomechanical stresses including inertial forces exerted on human body joints (Anderson et al. 2012). Given the motion and external force data, OpenSim performs inverse dynamics analysis with a multibody musculoskeletal system that has rigid skeletal bones with virtual markers, as shown in Figure 14, to calculate joint moments (Symeonidis et al. 2010). OpenSim is designed to conduct biomechanical simulation with experimental data, such as marker positions and kinematics obtained from marker-based motion capture systems. For this reason, the TRC file format that contains markers' geometric information is the only motion data format available in the current version of OpenSim.

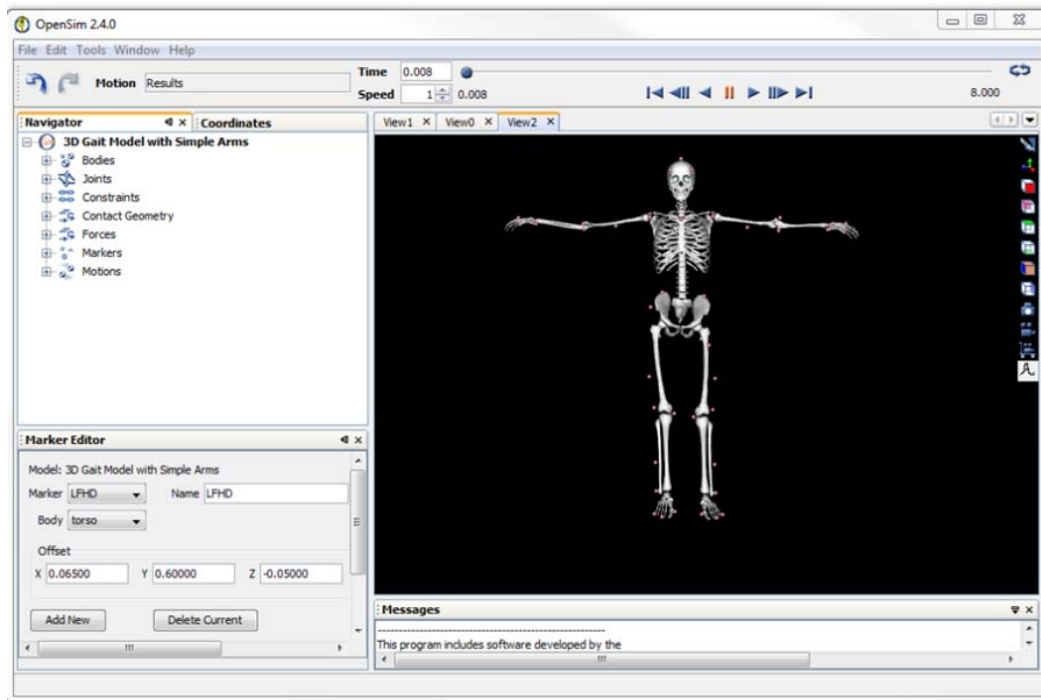


Figure 14. A screenshot of an OpenSim window and a multibody model with virtual markers

The procedures required to run OpenSim with marker data (i.e., TRC file) are as follows (Anderson et al. 2012): 1) scaling that adjusts both the mass properties (mass and inertia) and the dimensions of the body segment for the subject using the locations of markers; 2) inverse kinematics to both create motions in the body model by matching experimental markers with virtual markers, and to calculate joint angles; and 3) inverse dynamics that determines the net forces and torques at each joint that produces movement by solving the equations of motion with the given motion data (joint angles from inverse kinematics) and external force data. For scaling (adjusting anthropometric factors) and inverse kinematics (calculating body angles) processes, marker positions in the TRC marker data are the primary sources; however, such marker information is not available in the BVH motion data. To enable these two processes to be done with the motion capture data, we developed a user-friendly stand-alone system that automatically generates joint moments from motion capture data. This system is based on the OpenSim Application Programming Interface (API) to generate a human multibody model (.osim) with anthropometric and physical properties (e.g., body mass, center of mass, moment of inertia)

fitted to the subject, and a motion file (.mot) containing information on joint angles at each body joint from the BVH motion data; Figure 15 illustrates the overall workflow.

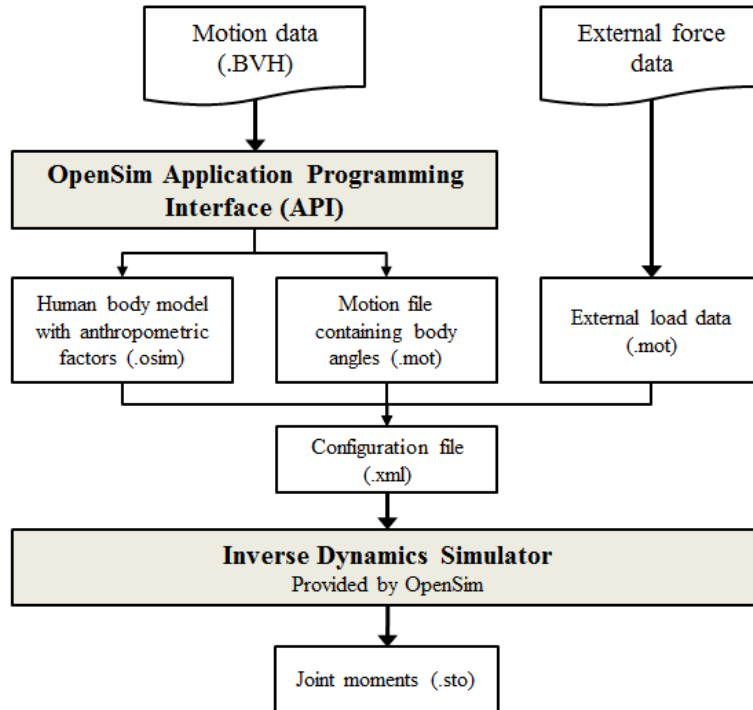


Figure 15. OpenSim workflow (Seo et al. 2014b)

First, the proposed system creates an OpenSim multibody model consisting of body segments and joints based on the hierarchical structures of bones and joints in the BVH motion data (Figure 16A). In addition, anthropometric parameters of the multibody model—such as mass, length, mass-center location, and moment-of-inertia of each body segment—are determined using a subject’s height and weight based on previous studies on these anthropometric parameters (Zatsiorsky et al. 1990; DeLeva 1996).

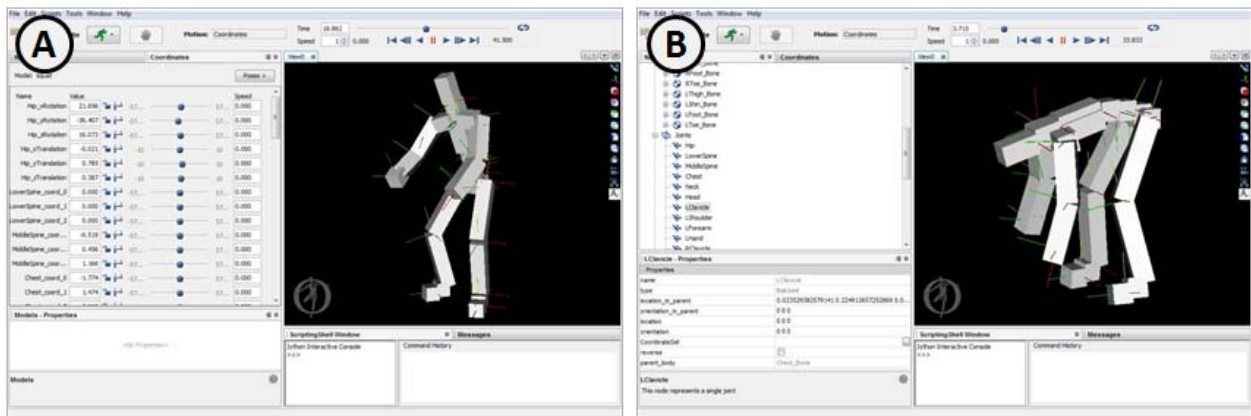


Figure 16. Multibody model from the BVH motion data. A: A multibody model with anthropometric parameters fitted to the subject. B: Represented motions in the multibody model based on the BVH motion data. (Seo et al. 2014b)

The next step is to generate a motion file (.mot) containing joint angles from the BVH motion data. Because both the BVH motion data and the motion file (.mot) in OpenSim define motions as joint rotations in degrees relative to the initial position of the joint, geometric information on skeleton structures from the BVH motion data are immediately written to the motion file in OpenSim (.mot). The multibody model that has motion information is shown in Figure 16B.

Once the OpenSim body model (.osim) and the motion file (.mot) are generated, the system also creates a configuration file (.xml) that will be used by the OpenSim inverse dynamics simulator to integrate the model (.osim), motion (.mot), and external force (.mot) files. The inverse dynamics simulator is an executable module built from the source codes for inverse dynamics from OpenSim, and thus enables us to perform inverse dynamics using the configuration file. The simulator saves the joint moments from dynamic biomechanical analysis to a storage file (.sto). These workflows are automatically processed only by inputting a subject’s anthropometric information (height and weight) and the BVH motion data in the stand-alone system.

Table 6. Comparison of anthropometric parameters from OpenSim and our approach (Seo et al. 2014b)

	Anthropometric Parameters	Existing approach	Our approach	% of Error
Upper arm	Mass (Kg)	1.96	1.97	-0.22%
	Length (m)	0.29	0.30	-5.43%
	Distance from center of mass to proximal joint as % of length	57.37%	57.72%	-0.62%
	Radius of gyration as % of length, transverse	26.73%	26.89%	0.61%
	Radius of gyration as % of length, longitudinal	15.70%	15.80%	0.60%
	Radius of gyration as % of length, frontal	0.28	0.29	0.60%
Lower leg	Mass (Kg)	3.50	3.30	5.71%
	Length (m)	0.43	0.42	2.30%
	Distance from center of mass to proximal joint as % of length	43.42%	44.58%	-2.69%
	Radius of gyration as % of length, transverse	27.11%	25.10%	-7.43%
	Radius of gyration as % of length, longitudinal	8.63%	10.20%	18.26%
	Radius of gyration as % of length, frontal	0.27	0.25	-9.89%

To verify the proposed approach, we collected motion data during ladder climbing from one male subject using an optical motion capture system, VICON™. The raw data captured from VICON™ was converted into the motion data in different file formats: .TRC and .BVH. Then, we compared anthropometric parameters and joint angles from our approach that uses BVH motion data with the parameters and angles from the existing approach of OpenSim that uses

TRC motion data. To measure the differences in anthropometric parameters, the percentage error between the values was used. For joint angles, we calculated the normalized root-mean-square errors (NRMSE) between the values from our approach and the ones from the existing approach during one cycle of climbing (240 frames, 2 seconds). As shown in Table 6, the differences in anthropometric parameters (except for the radius of gyration of a lower leg) were less than 5%. The radius of gyration is determined by the square root of the moment of inertia divided by the mass. Considering that only the dynamic rotational moment is affected by the value of the moment of inertia, the error in the inertial parameters of a lower leg would not significantly affect the joint moments at a knee joint. In addition, NRMSE values for body angles at elbows and knees were 0.079 and 0.081, respectively. These results indicate that the proposed approach accurately estimates anthropometric parameters and joint angles based on BVH motion data, compared with the values from the existing approach.

5.4 Results and Discussion

As a case study to show how on-site biomechanical analysis can be performed, we performed static biomechanical analysis using 3D SSPPTM with motion data obtained from vision-based motion capture and force data from force prediction models during ladder climbing (Seo et al. 2014a).

In 3D SSPPTM, joint moments at body joints can be presented by Percent Strength Capable (PSC: %), which means the percent of the population with sufficient strength. Strength Design Limit (SDL) and Strength Upper Limit (SUL) for joint moments correspond to the NIOSH Action Limit and Maximum Permissible Limit (NIOSH, 1981). The SDL was set at 99% for men and 75% for women, while the SUL was set at 25% for men and 1% for women.

The results indicate that there is no significant hazard on the back because back compression forces during ladder climbing are less than 500 N, as shown in Figure 17A. However, the PSC for joint moments at upper extremities (e.g., wrist, elbow, and shoulder) are below the SUL, which means that excessive joint moments could be exerted during ladder climbing (Figure 17B). Generally, a posture with a joint moment beyond the strength limit is hazardous because it can cause musculoskeletal injuries. In addition, excessive joint moments at upper extremities may increase the risk of falls from ladders. From this result, it is suggested that interventions to reduce musculoskeletal stresses on upper extremities should be implemented to prevent ladder-related injuries.

The results from the case study imply that, given motion capture data (e.g., BVH files), the motion data-driven biomechanical analysis provides a robust measure of internal forces. In addition, the usability issue of the proposed method is also important from a practical perspective in making the biomechanical models useful when performing ergonomic evaluations during tasks. In this context, it should be clear that the automatic processes of motion data obtained directly from work places enable ergonomists and practitioners to identify stressful climbing behaviors by evaluating internal loading conditions in a timely manner without technical sophistication or skill.

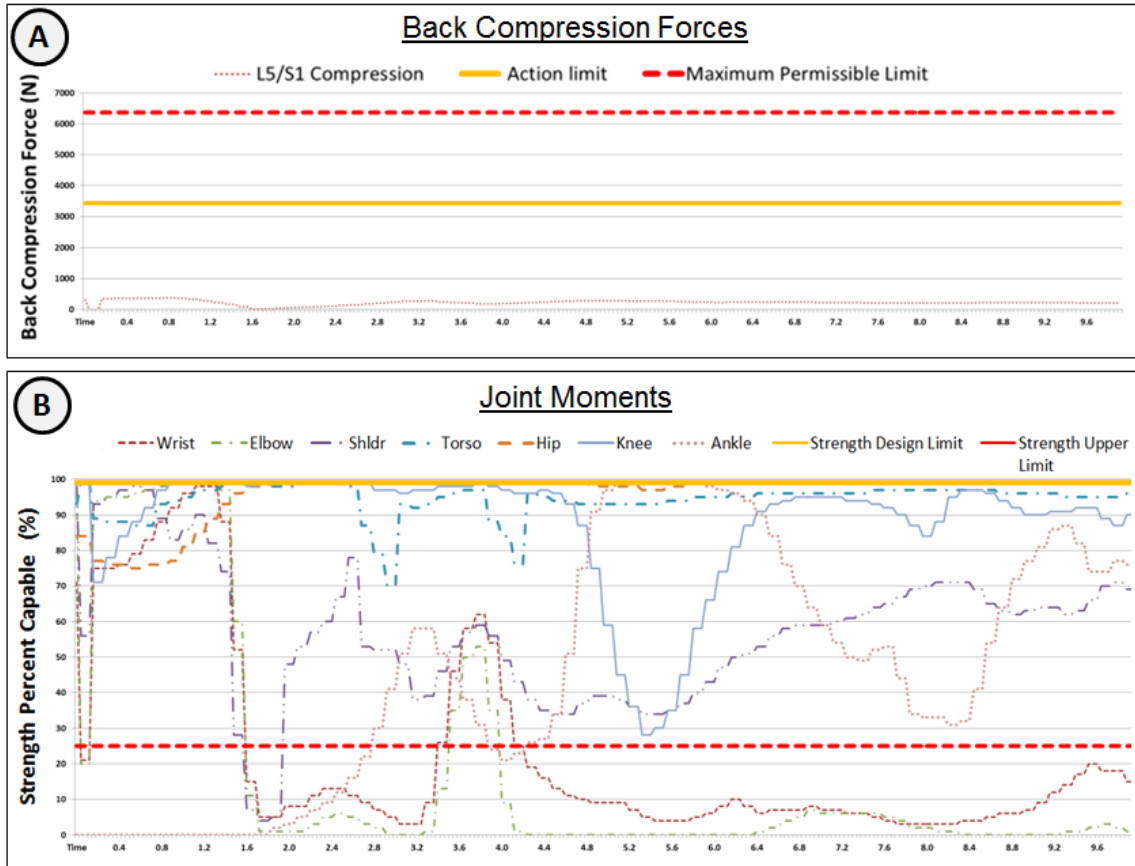


Figure 17. Biomechanical analysis results during ladder climbing. A: Back compression force (N). B: Strength percent capable (%) of body joints. (Seo et al. 2014a)

6. PROTOTYPE OF A FIELD TOOL FOR ON-SITE BIOMECHANICAL ANALYSIS DURING LADDER CLIMBING

6.1 Aim of Field Tool

By combining proposed methodologies for the data collection and automated data processing for biomechanical analysis described in Sections 3–5, we developed a field tool for on-site biomechanical analysis during ladder climbing. A custom software solution—hereby referred to as the “field tool”—was developed to afford an effective utilization of the visual, kinematic, and ergonomic data generated by the proposed on-site biomechanical analysis system. The field tool displays the video stream and kinematic skeletal model recorded during on-site motion capturing alongside the derived biomechanical data. These data are temporally synchronized to one another and presented in a user-friendly visual format. This allows for an effective and intuitive interpretation of a particular action or posture taken by a worker during recording and the action’s or posture’s impact on health and safety during ladder climbing. In addition, the proposed tool will be useful for providing feedback to workers about their climbing behaviors when meeting with workers during breaks, at the end of the shift, or during scheduled safety meetings.

One thing to note is that this field tool uses an existing biomechanical analysis tool in order to make the tool flexible enough to adopt any other biomechanical software. In this version of the prototype, we used 3D SSPP™, and thus 3D SSPP™ should be installed in the computer where this field tool is installed. The field tool is flexible enough to be used with other biomechanical analysis tools with minor adjustment.

6.2 System Architecture

To build the field tool, C# was chosen as a primary language due to its power and ease-of-use in creating dynamic and intuitive Graphical User Interfaces (GUIs). Because C# incorporates the Microsoft .NET Framework, efficient communication is possible between the field tool and other managed software systems developed for the proposed approach.

Modern object-oriented software engineering methodologies were observed to ensure expandability, particularly linear inheritance schemes and encapsulation. Additionally, design patterns were employed that afford the easy modification of software components, particularly those for which the programming methodologies used are dependent on the data sources. This ensures that the field tool can be quickly revised to account for modifications or upgrades from future research. This prototype was basically designed only for static biomechanical analysis (3D SSPP™) at this time. However, it can be easily extended for dynamic biomechanical analysis by incorporating the automated motion data processing for OpenSim suggested in Section 5.

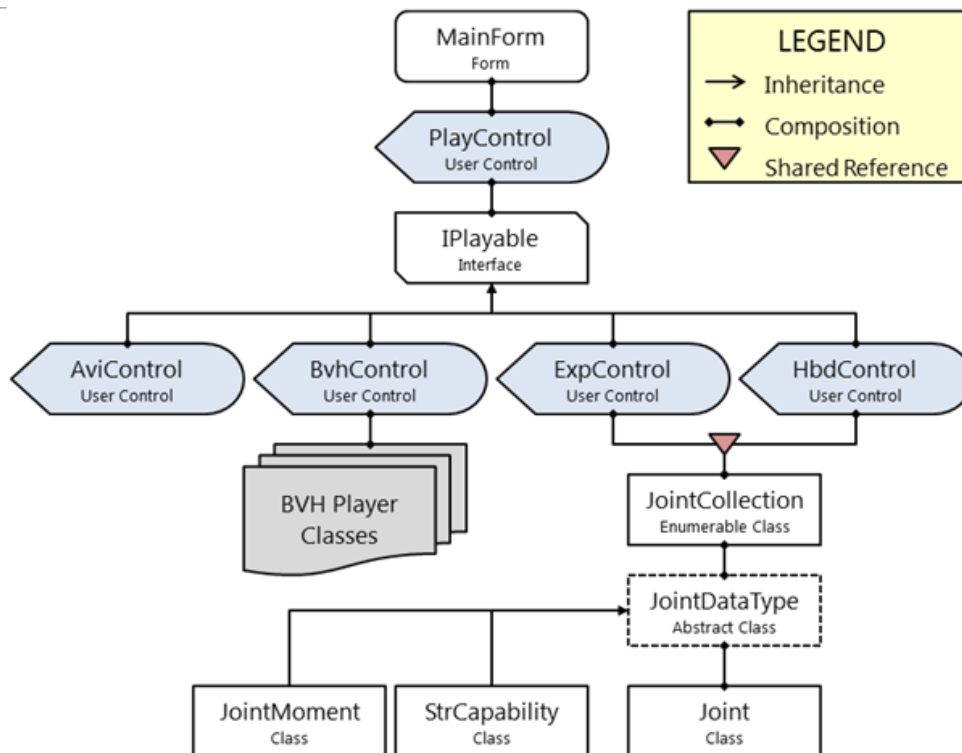


Figure 18. Partial class diagram representing field tool architecture

A class diagram (flow chart outlining the relationships between objects in a program) for the field tool is provided in Figure 18. The GUI is divided into five major components, each of

which is encapsulated within a C# User Control. *AviControl* (video player), *BvhControl* (motion capture player), *ExpControl* (biomechanical data graph), and *HbdControl* (color-coded joint stress indicator diagram) each implement the interface *IPlayable*. This allows for predefined commands to be issued in a consistent manner to any of the user controls responsible for handling visual feedback. These commands are executed by a fifth user control, *PlayControl*, which is composed of the four *IPlayable* controls. *PlayControl* contains the GUI components responsible for playback manipulation (e.g., play, pause, and seek). The *IPlayable* interface affords iteration and temporal synchronization of the user controls it is composed with, and allows for future playback components to be added and synchronized with minimal effort (so long as those components properly implement the *IPlayable* interface).

An enumerable collection class, *JointCollection*, is used to store biomechanical data from 3D SSPP™. The collection is composed of objects derived from *JointDataType*, an abstract class that defines the manner in which biomechanical data are stored and labeled. *JointDataType* is itself a collection class composed of *Joint* objects, which store the values associated with a particular type of biomechanical data. To create a new type of biomechanical data that can be graphed in the *ExpControl* panel, *JointDataType* is inherited from biomechanical data, and certain parameters (e.g., data types, labels, and tolerances used to color the indicators in *HbdControl*) are overridden. This inheritance scheme allows for the manipulation of and amendment to the types of biomechanical data displayed in the field tool.

Additionally, *JointCollection* utilizes a factory design pattern to read biomechanical data from text files. A modifiable XML document is used to define each type of data and the indexing information necessary for accessing it. This technique ensures that the field tool can be quickly modified to accept biomechanical data from different sources (e.g., 3D SSPP™ and *OpenSim*) so long as those data are outputted in standard text file format.

6.3 System Components

The field tool is divided into three major visualization components: video playback, kinematic modeling, and biomechanical feedback. Although existing solutions are available for each individual component, the field tool's novelty stems from the combination and synchronization of the three. This consolidation makes the field tool a powerful utility for analyzing the data produced by the proposed system.

A screenshot of the field tool with its visualization components labeled is shown in Figure 19. At the top-left corner of Figure 19 is the video player (outlined in orange), which displays the original video stream recorded during motion capture. Its inclusion ensures that workers and scenes can be readily identified and differentiated. Additionally, it allows for visual confirmation that the kinematic model produced by the motion capture system is a reasonable skeletal representation (i.e., that no problems occurred during pose estimation at a particular time frame that would result in erroneous biomechanical data).

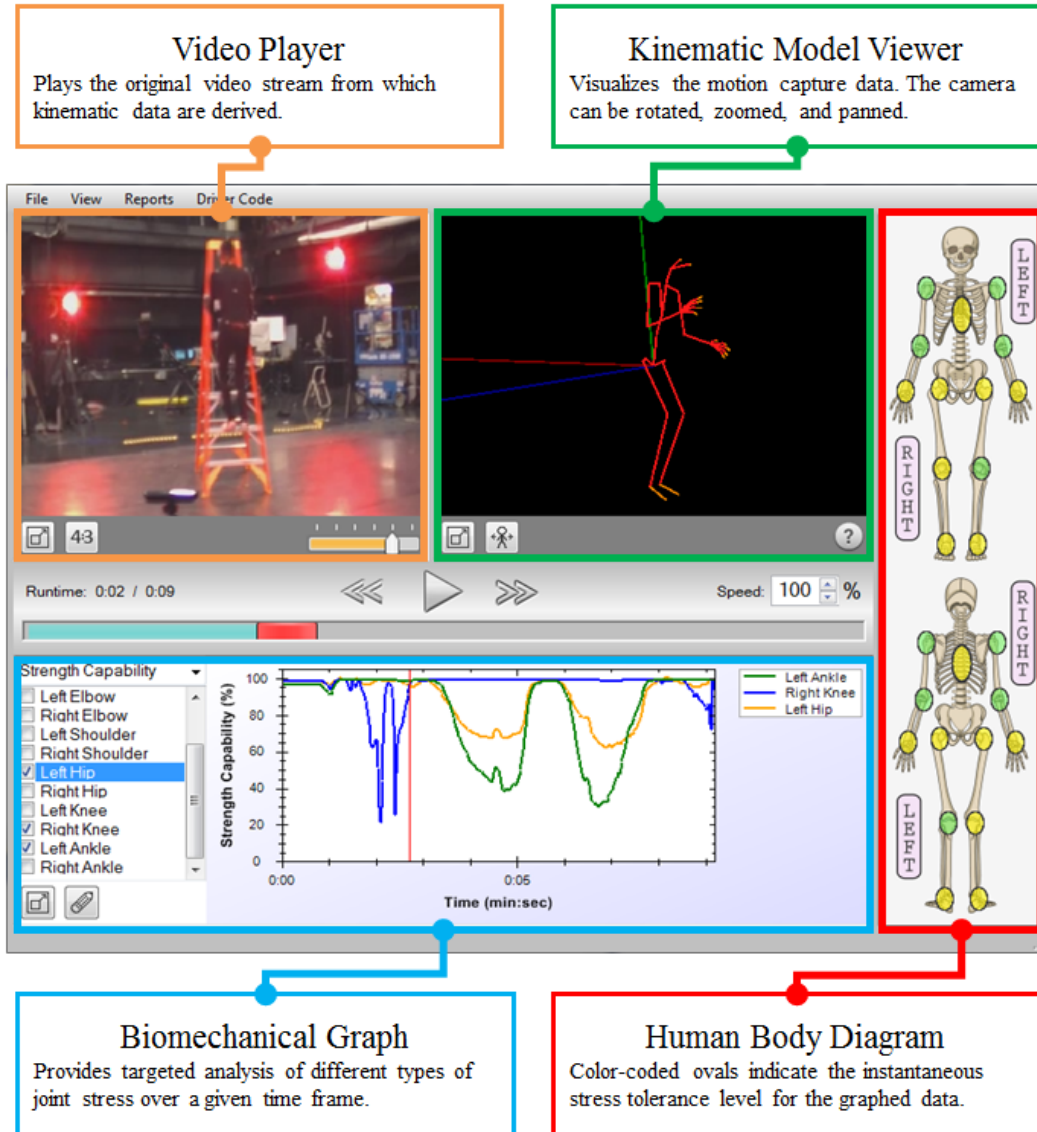


Figure 19. Screenshot of field tool with labeled visualization components

To the right of the video player, outlined in green in Figure 19, is a viewer for the kinematic model produced by the vision-based motion capture data derived from the recorded video. Playback of the animated motion capture data is synchronized with the video stream displayed alongside it. The camera in this view can be rotated, panned, and zoomed to allow the user optimal comprehension of the postures and motions that result in particular bodily stresses.

The biomechanical data graph can be seen at the bottom of Figure 19 outlined in blue. The graph allows the user to plot different types of ergonomic strain (e.g., joint moment or strength capability) for specific joints obtained from biomechanical analysis tools such as 3D SSPP™. A moving vertical red line on the plot corresponds with the point in time for the current frame displayed in the video player and kinematic modeler. This allows for playback to be paused at points in time where peaks or valleys occur within the graph, and for the corresponding frame of the video and motion capture model to be analyzed to determine what caused that particular hazardous musculoskeletal stresses. The data plot can be zoomed and panned with simple mouse

commands, allowing the user to focus their attention on a time frame within the recording session in which a specific posture or motion takes place.

A human skeletal diagram with color-coded joint stress level indicators is shown at the far right side of Figure 19. The ovals at each key joint change color from green to yellow to red, indicating the predefined joint stress tolerance level for the particular type of biomechanical data (In this prototype, the biomechanical data and tolerance level are obtained from 3D SSPP™.) currently being graphed. These indicators are always visible for every joint, ensuring that extreme spikes in stress levels do not go unnoticed by the user due to that particular joint not having been plotted.

6.4 Discussion

The field tool has shown itself to be an effective utility for interpreting the data produced by the proposed on-site biomechanical analysis system. It has been successfully used to analyze empirical data recorded using the proposed system's components, and these analyses have provided invaluable ergonomic and biomechanical information associated with specific poses and actions. Utilizing the field tool with video, kinematic models, and biomechanical data derived from real-world construction worker behaviors during ladder climbing will provide construction firms and researchers with a powerful means of evaluating and understanding the potential health and safety risks associated with specific postures and motions.

Although the results thus far have been positive, there are further enhancements and additions that will be made in order to increase the efficacy of the field tool. Currently, the video, kinematic data, and biomechanical data are each produced separately and are individually loaded into the field tool. As such, care must be taken by the user to ensure that all of these components are valid and properly synchronized. Plans for future works include the development of a server-side utility for generating these data and uploading them to the tool. The video recording, marker-less motion capture, and biomechanical analysis processes will be controlled by a centralized software system. This system will synchronize these data with one another and package them into a single binary file. The field tool will interface with this server-side system, and the binary files will be listed for the user. The user will then select the recording of interest and all of the data will be downloaded and displayed automatically. This process will allow users to make effective use of the proposed system with minimal training and with little risk of incorrect assessments due to improperly correlated data.

Additional usability enhancements of the field tool are planned as well. At the moment, the color-coded joint stress level indicators in the human body diagram panel only provide information relating to instantaneous strain. These will be upgraded in the future to indicate potential ergonomic dangers associated with repeated low-level stresses over extended periods of time. Additionally, the GUI will be updated with a color-coded bar alongside the playback slider to indicate periods of time in which excessive stresses were recorded. This will allow users to discover postures that could potentially result in injury quickly, without having to analyze the entire recorded time period. A second slider bar will be added beneath the playback bar to allow the user to select a region of interest (time frame) for analysis. The selected time frame will be looped during playback, providing a means of more easily analyzing specific motions taken by the subject during the recording session.

7. CONCLUSIONS AND FUTURE RESEARCH

7.1 Vision-based Motion Capture

We tested vision-based motion capture algorithms using 2D images from multiple cameras (or a 3D camcorder) and 3D images from a stereo vision camera system to collect 3D skeleton-based motion data during ladder climbing. The multiple camera-based approach uses 2D images from video cameras with different viewpoints, and relies on 2D pose estimation and 3D reconstruction algorithms to extract 3D skeleton-based motion data from the 2D images. The stereo vision camera-based approach provides a more simplified solution to collect motion data because it can extract 3D skeleton-based motion data directly from 3D images. These vision-based motion capture approaches are considered an attractive solution to the limitations on optical motion capture approaches that use markers attached to workers when collecting motion data under real conditions.

We conducted a case study to test the feasibility of the use of vision-based motion capture approaches. The results showed that these approaches are promising for the collection of motion data during ladder climbing under real conditions. However, the accuracy of motion data should be further improved to obtain reliable biomechanical analysis results using the motion data. The case study revealed that vision-based approaches face limitations in tracking upper extremities due to self-occlusions. Further studies are needed to both minimize self-occlusions and increase the accuracy. It appears that the positions of cameras with clear viewpoints on workers would be critical. By testing different positions of cameras and comparing the accuracy, optimal positions of cameras can be recommended. In addition, the use of additional cameras should be examined to determine whether additional cameras can provide better results for motion capture.

7.2 External Forces During Ladder Climbing

For biomechanical analysis, the measurement of external forces—such as hand and foot forces—is essential. Although previous biomechanical studies have relied on force measurement devices, on-site biomechanical analysis requires a robust estimation of external forces because direct measurement is rarely possible under real conditions. Based on the hypothesis that force profiles exerted on hands and feet during ladder climbing have similar patterns if factors involved in ladder climbing activities are the same, we explored experimental force data-driven prediction by modeling force profiles obtained from laboratory experiments.

We tested the feasibility of the proposed estimation method, and found that force prediction models performed well in estimating hand and foot forces during ladder climbing. However, the linear model that assumed multiple polylines on force profiles for simplification may not work well for fitting the model with the actual profiles that have a lot of variation in curves. On the other hand, the polynomial regression model captured dynamic patterns in force profiles better than the linear model. However, it may not perform well to capture forces during the stabilizing period when the forces are relatively constant. To improve the accuracy of external force prediction during ladder climbing, further studies should be performed to examine diverse fitting algorithms.

In addition, in this study, we tested the proposed method only in specific conditions (e.g., portable step ladder, diagonal climbing style). For future research, extensive laboratory experiments need to be conducted to collect hand and foot forces by varying factors affecting

forces identified from literature, to determine dominant factors through statistical analysis, and to develop force prediction models that enable us to predict hand and foot forces under diverse conditions during ladder climbing.

7.3 Motion Data–Driven Biomechanical Analysis

We proposed on-site biomechanical analysis during ladder climbing based on motion data collected directly from construction sites. However, motion data from vision-based approaches is not compatible with existing computerized biomechanical analysis tools. To address this issue, we suggested a semi-automated process to convert the motion data into available data and represent motions in biomechanical analysis tools such as 3D SSPPTM and OpenSim. The results from a case study during ladder climbing show that the proposed method for motion data processing was successfully used to perform biomechanical analysis using vision-based motion data. For future research, the suggested procedures for on-site biomechanical analysis should be incorporated in the field tool, and thus using only the single user interface, users can evaluate ladder climbing behaviors exhibited by workers.

7.4 A Field Tool for On-Site Biomechanical Analysis

We developed the field tool for on-site biomechanical analysis using vision-based motion capture data and the estimation of external forces during ladder climbing. The field tool displays visual, kinematic, and ergonomic data at the same time, and thus provides not only an effective and intuitive interpretation of biomechanical analysis results to practitioners or field managers, but also visualized feedback to workers on their climbing styles that may produce excessive internal loads during ladder climbing.

The field tool developed in this project is a prototype for a static biomechanical analysis. Further research should be performed to revise and upgrade existing functionalities. Considering the possibility for modifications, we designed system architecture to be quickly revised for different sources (e.g., 3D SSPPTM and OpenSim).

7.5 Comprehensive Validation

Validation is essential for applying the developed approach to real applications. However, comprehensive validation of the proposed field tool has not been fully conducted. Comprehensive validation can be performed by comparing biomechanical analysis results from our approaches and laboratory experiments that use optical motion capture systems and direct force measurement systems. In addition, the usability and practicality of the proposed prototype of the field tool needs to be further studied by conducting case studies in the diverse conditions of construction sites.

8. REFERENCES

- Aminian, K., and Najafi, B. (2004). "Capturing human motion using body-fixed sensors: outdoor measurement and clinical applications." *Computer Animation and Virtual Worlds*, 15(2), 79–94.
- Anderson, F. C., Delp, S., DeMers, M., Guendelman, E., Habib, A., Hamner, S., Hicks, J., Higginson, J., John, C., van der Krogt, M., Ku, J., Liu, M., Lund, K., Loan, P., Reinbolt, J. Seth, A., and Sherman, M. (2012). *OpenSim user's guide*. <<https://opensim.stanford.edu>>
- Armstrong, T. J., Ashton-Miller, J., Wooley, C., Kemp, J., Young, J. and Kim, H. (2008). *Development of Design Interventions for Preventing Falls from Fixed Ladders*. CPWR Technical Report.
- Ayoub, M. M. and Bakken, G.M. (1978). *An ergonomic analysis of selected sections in Subpart D, walking and working surfaces*. Institute for Biotechnology, Texas Tech University, TX.
- Bloswick, D. S., and Chaffin, D. B. (1990). "An Ergonomic Analysis of the Ladder Climbing Activity." *International Journal of Industrial Ergonomics*, 6, 17–27.
- Bureau of Labor Statistics (2011) *National Census of Fatal Occupational Injuries in 2010*. USDL-11-1247 (http://www.bls.gov/news.release/archives/cfoi_08252011.pdf)
- Bureau of Labor Statistics (2012) *NONFATAL OCCUPATIONAL INJURIES AND ILLNESSES REQUIRING DAYS AWAY FROMWORK*, 2011. USDL-12-2204 (<http://www.bls.gov/news.release/pdf/osh2.pdf>)
- Center for Construction Research and Training (CPWR) (2013). *The Construction Chart Book: The U.S. Construction Industry and Its Workers (Fifth Edition)*. <<http://www.cpwr.com/publications/construction-chart-book>> (April, 2013)
- Chapman, A.E. (2008). *Biomechanical Analysis of Fundamental Human Movement*. Human Kinetics, IL.
- Davis, R. B., Ounpuu, S., Tyburski, D., and Gage, J. R. (1991). "A gait analysis data collection and reduction technique." *Human Movement Science*, 10(5), 575–587.
- DeLeva, P. (1996). "Adjustments to Zatsiorsky-Seluyanov's segment inertia parameters." *Journal of Biomechanics*, v.29 (9), pp.1223–1230.
- Delp, S. L., Anderson, F. C., Arnold, A. S., Loan, P., Habib, A., John, C. T., and Thelen, D. G. (2007). "OpenSim: open-source software to create and analyze dynamic simulations of movement. *Biomedical Engineering*." *Biomedical Engineering, IEEE Transactions on*, 54(11), 1940–1950.
- Dewar, M.E. (1977). "Body movements in climbing a ladder." *Ergonomics*, 20(1), 67–78.
- Häkkinen, K. K., Pesonen, J. and Rajamäki, E. (1988). "Experiments on Safety in the Use of Portable Ladders." *Journal of Occupational Accidents* 10(1): 1–19.
- Hammer, W., and Schmalz, U. (1992). "Human Behavior when Climbing Ladders with Varying Inclinations." *Safety Science*, 15, 21–38.
- Han, S., Achar, M., Lee S., and Peña-Mora, F. (2012). "Automated 3D human skeleton extraction using range cameras for safety action sampling." *Proceedings of the 12th International Conference on Construction Applications of Virtual Reality (ConVR)*, Taipei, Taiwan.

- Han, S., and Lee, S. (2013). "A Vision-based Motion Capture and Recognition Framework for Behavior-based Safety Management." *Automation in Construction*, 35,131–141.
- Hartley, R., and Zisserman, A. (2000). *Multiple view geometry in computer vision (Vol. 2)*. Cambridge.
- Hoozemans, M. J., de Looze, M. P., Kingma, I., Reijneveld, K. C., de Korte, E. M., van der Grinten, M. P., and van Dieën, J. H. (2005). "Workload of window cleaners using ladders differing in rung separation." *Applied ergonomics*, 36(3), 275–282.
- Kassir, A., and Peynot, T. (2010). "Reliable automatic camera-laser calibration." In *Australasian Conference on Robotics and Automation*.
- Kumar, S. (1999). *Biomechanics in Ergonomics*. Taylor & Francis Inc., Philadelphia, US.
- Lee, Y.H., Cheng, C.K., and Tsuang, Y.H. (1994). "Biomechanical analysis in ladder climbing: the effect of slant angle and climbing speed." *Proceedings of the National Science Council*, 18(4), 170–178.
- Liu, C., Yuen, J., and Torralba, A. (2011). "Sift flow: Dense correspondence across scenes and its applications." *Pattern Analysis and Machine Intelligence, IEEE Transactions on*, 33(5), 978–994.
- McIntyre, D.R. (1983). "Gait Patterns During Free Choice Ladder Ascents." *Human Movement Science* 2(3): 187–195.
- Meredith, M., and Maddock, S. (2001). *Motion capture file formats explained*. Department of Computer Science, University of Sheffield.
- Moeslund, T. B., and Granum, E. (2001). "A survey of computer vision-based human motion capture." *Computer Vision and Image Understanding*, 81(3), 231–268.
- Moeslund, T. B., Hilton, A., and Krüger, V. (2006). "A survey of advances in vision-based human motion capture and analysis." *Computer Vision and Image Understanding*, 104(2), 90–126.
- National Institute for Occupational Safety and Health (NIOSH) (1981). *Work Practices Guide for Manual Lifting*. Technical report number: 81–122, U.S. Dept. of Health and Human Services, Cincinnati, Ohio.
- Perry, M. J., and Ronk, C. J. (2010). *Preventing Falls from Ladders in Construction*. Harvard School of Public Health, Department of Environmental Health.
- Poppe, R. (2007). "Vision-based human motion analysis: An overview." *Computer Vision and Image Understanding*, 108(1), 4–18.
- Radwin, R. G., Marras, W. S., and Lavender, S. A. (2001). "Biomechanical aspects of work-related musculoskeletal disorders." *Theoretical Issues in Ergonomics Science*, 2(2), 153–217.
- Seo, J., Han, S., Lee, S., and Armstrong, T. J. (2014a). "Feasibility of On-Site Biomechanical Analysis During Ladder Climbing." 2014 Construction Research Congress (2014 CRC). (accepted).
- Seo, J., Starbuck, R., Han, S., Lee, S., and Armstrong, T. J. (2014b). "Motion-Data-driven Biomechanical Analysis During Construction Tasks on Sites." *Journal of Computing in Civil Engineering* (submitted).

Shotton, J., Sharp, T., Kipman, A., Fitzgibbon, A., Finocchio, M., Blake, A., and Moore, R. (2013). "Real-time human pose recognition in parts from single depth images." *Communications of the ACM*, 56(1), 116–124.

Smith, G.S., Timmons, R.A., Lombardi, D.A., Mamidi, D.K., Matz, S., Courtney, T.K. and Perry, M.J. (2006). "Work-related ladder fall fractures: Identification and diagnosis validation using narrative text." *Accident Analysis and Prevention*, 38, 973–980.

Starbuck, R., Seo, J., Han, S., and Lee, S. (2014). "A Stereo Vision-based Approach to Markerless Motion Capture for On-Site Kinematic Modeling of Construction Worker Tasks." *International Conference on Computing in Civil and Building Engineering-2014* (submitted)

Symeonidis, I., Kavadarli, G., Schuller, E., and Peldschus, S. (2010). "Simulation of Biomechanical Experiments in OpenSim." In *XII Mediterranean Conference on Medical and Biological Engineering and Computing 2010*, Springer Berlin Heidelberg, 107–110.

Uijlings, J. R., Smeulders, A. W., and Scha, R. J. (2010). "Real-time visual concept classification." *Multimedia, IEEE Transactions on*, 12(7), 665–681.

Weerasinghe, I. P. T., Ruwanpura, J. Y., Boyd, J. E., and Habib, A. F. (2012). "Application of Microsoft Kinect sensor for tracking construction workers." *Proceeding of 2012 Construction Research Congress (CRC)*, West Lafayette, IN, 858–867.

Yang, Y., and Ramanan, D. (2009). "Articulated pose estimation with flexible mixtures of parts." *Proceedings of the 2011 IEEE Conference on Computer Vision and Pattern Recognition*, Colorado Springs, USA.

Zatsiorsky, V. M., Seluyanov, V. N., and Chugunova, L. G. (1990). "Methods of determining mass-inertial characteristics of human body segments." *Contemporary problems of biomechanics*, 272–291.

9. APPENDIX

9.1 User’s Manual for the Field Tool

FIELD TOOL USER MANUAL

The field tool provides users with a means of reviewing and interpreting data produced by marker-less motion capture-based biomechanical analysis systems. It is intended for use with systems that derive kinematic and biomechanical data from video and/or depth sensor recordings.

The field tool does not evaluate the accuracy the motion capture-based data—it is the user’s responsibility to ensure the efficacy of data collection methods. Users should be adequately trained in using the systems by which the data analyzed by the field tool is produced. Additionally, the field tool is not an instructional device for biomechanical and ergonomic data analysis. It is up to the user to interpret the data displayed in the system, for which prerequisite background information will be required.

1. Overview of the GUI

The field tool’s graphical user interface (GUI) was designed for simplicity and ease-of-use. Users should be able to familiarize themselves with its interfacing capabilities relatively quickly. When the field tool is first started, users will be greeted with a window similar to the one shown in Figure 1.

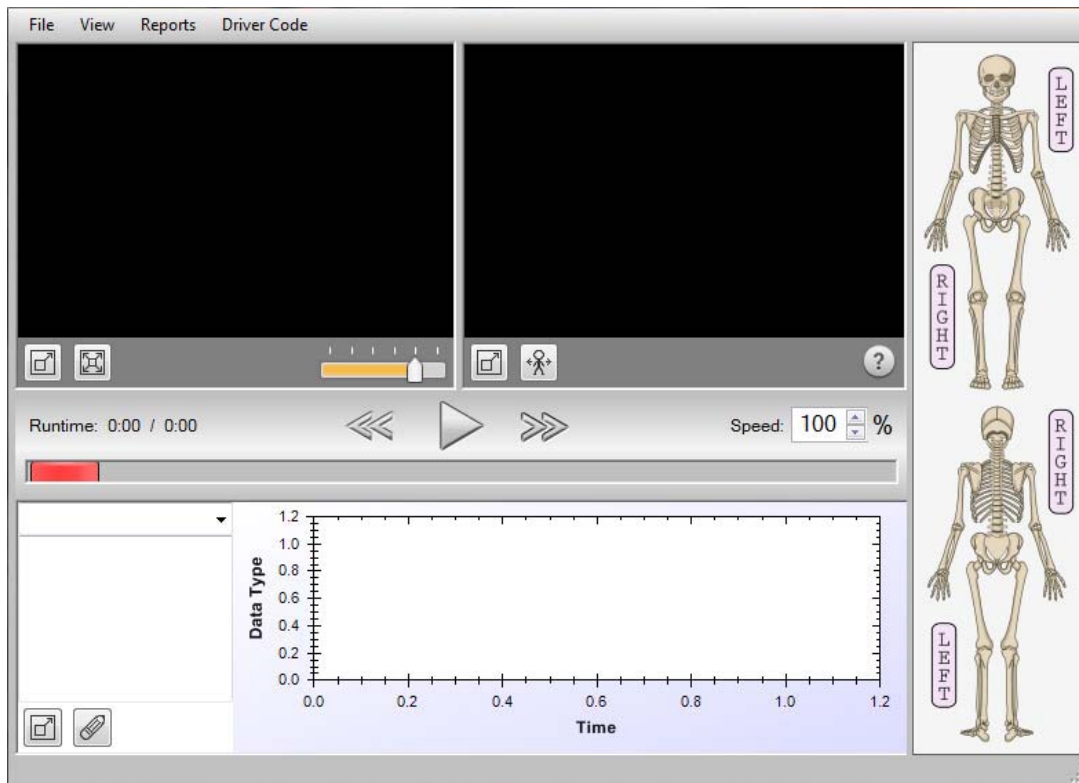


Figure 1. Field tool after initial launch

The GUI is divided into five major components: playback controller, video player, motion capture viewer, biomechanical data graph, and body diagram. These components, with the exception of the playback controller, can be resized by clicking and dragging on the borders of each panel. The locations of these borders are outlined in Figure 2, which shows the main window after panel resizing (the direction of the resizes are indicated with arrows).

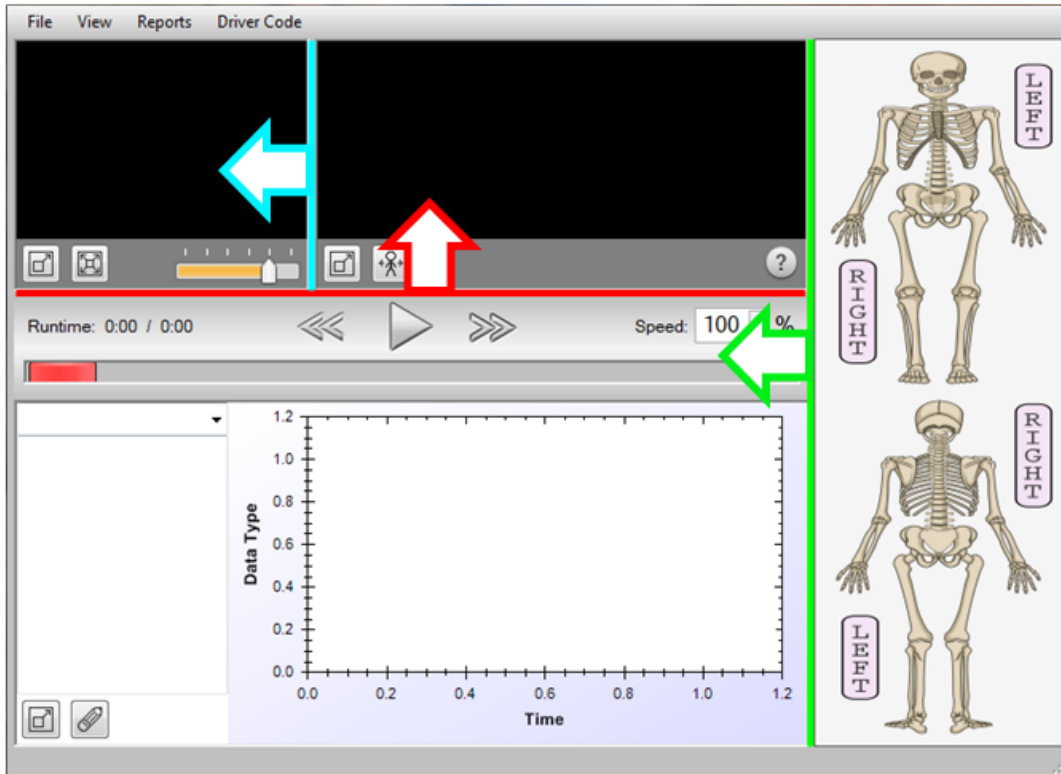


Figure 2. Resized field tool with resizing bars highlighted

2. File Loading

Files produced by marker-less motion capture-based biomechanical analysis systems must be loaded into the field tool individually. There will be three files that will be loaded in order to perform an analysis: a video file, a motion capture file, and a biomechanical data file.

First, click **File** at the top-left corner of the screen in the main menu strip and scroll to **Open**. A fold-out menu will appear giving options for opening the three necessary file types. This menu is shown in Figure 3.

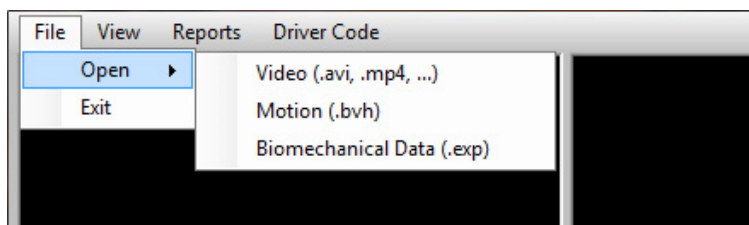


Figure 3. File opening menu

Select **Video (.avi, .mp4, ...)** from the menu. A new file dialog box will appear. Browse to the location on your hard drive's file structure where the video file associated with the desired recording session is located. Select the file and press **Open**. This process is shown in Figure 4.

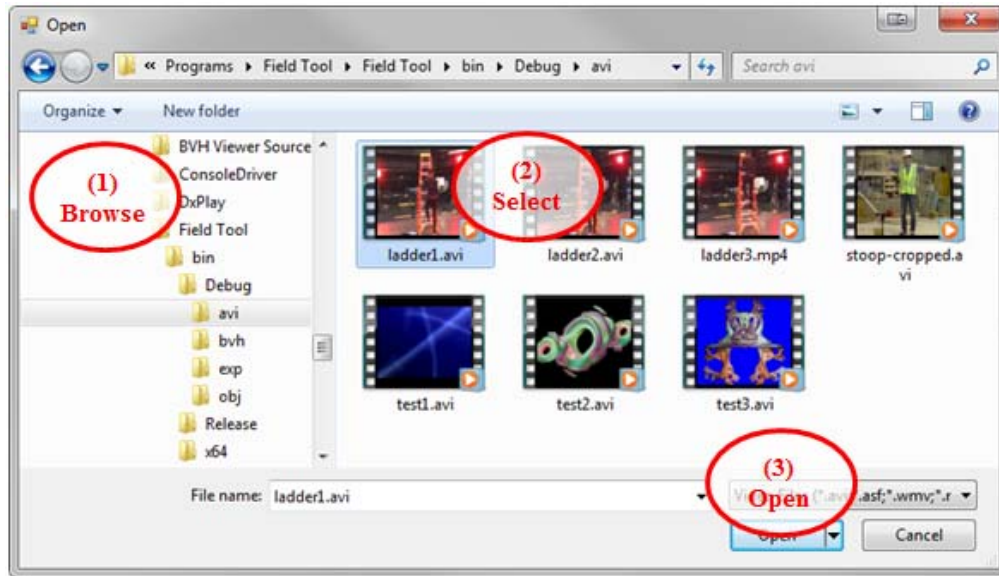


Figure 4. File dialog

If the video file is of a non-standard type, it may not be displayed in the menu; however, the field tool may still be able to successfully open it. Click the drop-down menu at the bottom-right corner of the file dialog (above the **Open** and **Cancel** buttons) and select **All Files (*.*)**, as shown in Figure 5. The file will then appear in the dialog.

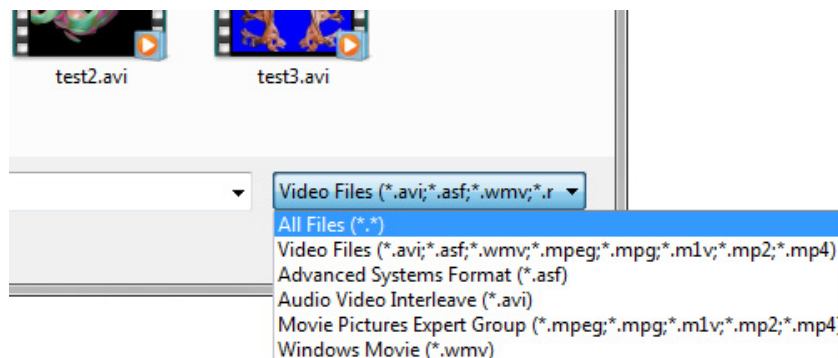


Figure 5. File type selection menu in file dialog

Once a video file is opened, it will appear in the top-left panel on the main window. Repeat this process for the motion capture and biomechanical files by selecting **Motion (.bvh)** and **Biomechanical Data** in the **Open** menu, respectively. These three files must all be from the same recording session and temporally synchronized.

After loading all three files, the main window will look similar to the one shown in Figure 6.

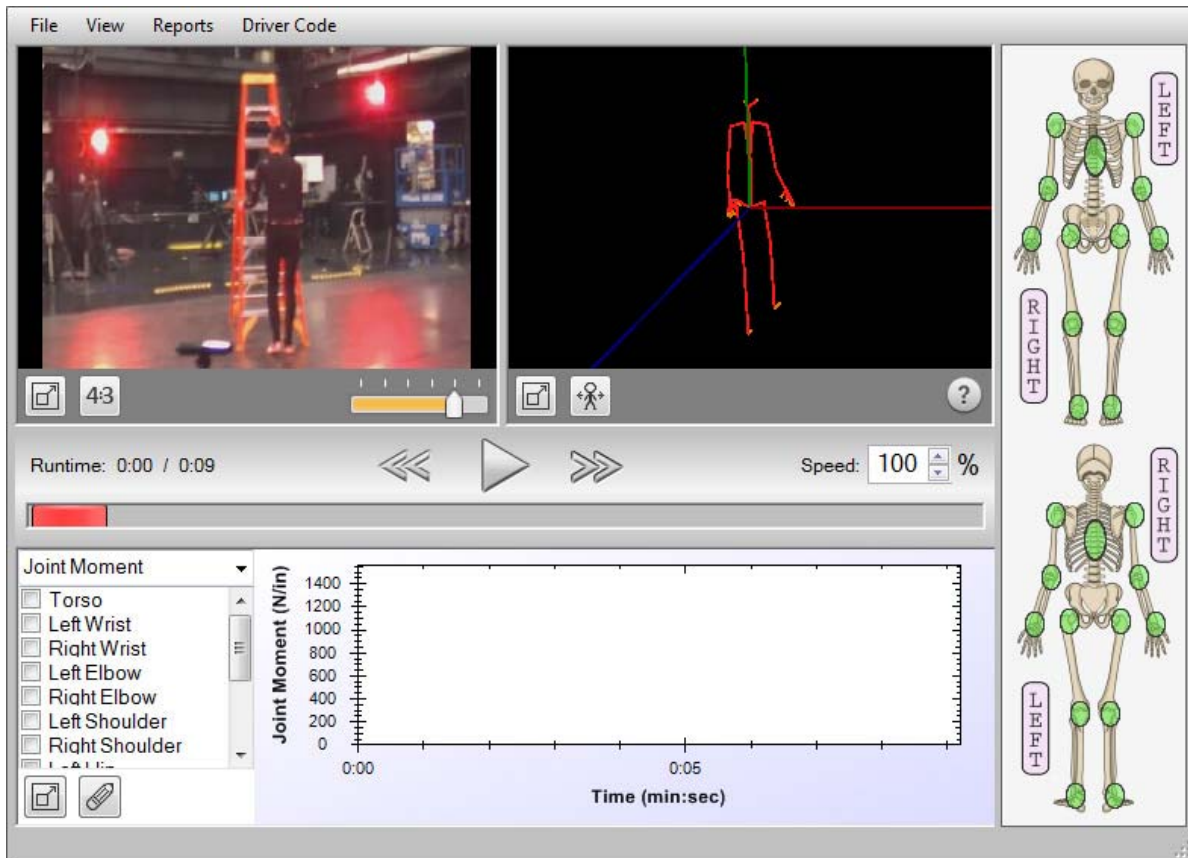


Figure 6. Main window after loading video, motion capture, and biomechanical data files

3. Playback Control Panel

After loading one or more files, playback can be controlled using the panel at the middle of the main window, shown in Figure 7.



Figure 7. Playback controller panel

The field tool synchronizes the video, motion capture, and biomechanical data files automatically. The playback control panel will control all three files. To play or pause, click the button at the center of the panel. To seek the play time forward or backward, click and drag the red box inside of the bar at the bottom of the panel. The playback speed can be changed by clicking the up and down arrows in the scroll box located at the upper-right corner of the panel. All of these features are labeled in Figure 7.

4. Video Player Panel

The video player panel, shown in Figure 8, displays the video recorded during motion capture. This panel is useful for visually comparing the actual postures of the recorded subject with those derived by the marker-less motion capture system (see Section 5, Motion Capture Panel) to ensure that there were no significant errors during pose estimation. It can also be useful for quickly identifying workers, scenes, and objects that aren't detected by the marker-less motion capture system.

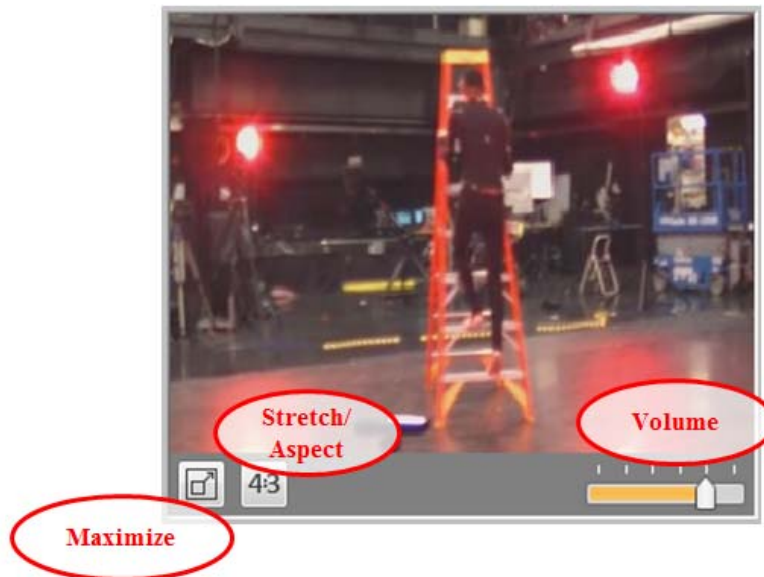


Figure 8. Video player panel

At the bottom-left corner is a button that maximizes the video panel. The button to its right switches between stretch mode, which forces the video to fill the viewing window, and aspect ratio mode, which maintains the video file's height and width proportionality. The slider at the bottom-right corner of the panel controls the volume of the audio stream for the video file. All of these features are labeled in Figure 8.

5. Motion Capture Panel

The motion capture panel is located to the right of the video panel. It displays the motion capture data derived from the video and/or depth data derived via marker-less motion capture. It is useful for analyzing postures and movements of recorded subjects for comparison with biomechanical data (see Section 6, Biomechanical Data Graph Panel) for interpreting the impact that specific poses have on worker health. Figure 9 shows the default view of the motion capture panel.

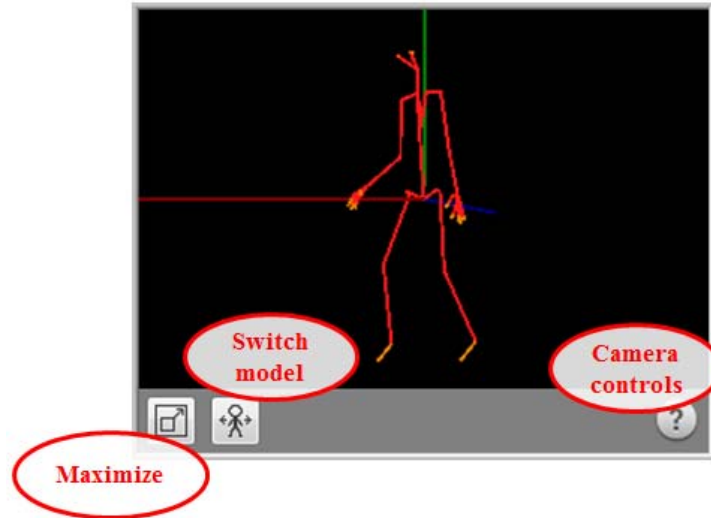


Figure 9. Motion capture panel

The button at the bottom-left corner maximizes the viewing window. The button to its right switches the view between two different model styles, the second of which is shown in Figure 10. The icon at the bottom-right corner provides the user with a description of the available camera control commands, which are listed in Table 1:

Table 1. Camera control commands for the motion capture panel.

Action	Command
Rotate camera	Hold left mouse button and drag left/right/up/down
Zoom camera	Hold right mouse button and drag up/down
Roll camera	Turn mouse wheel up/down

Don't worry about having to memorize Table 1—hovering over the icon at the bottom-right corner of the motion capture panel displays a small box with a listing of these commands, as shown in Figure 10.

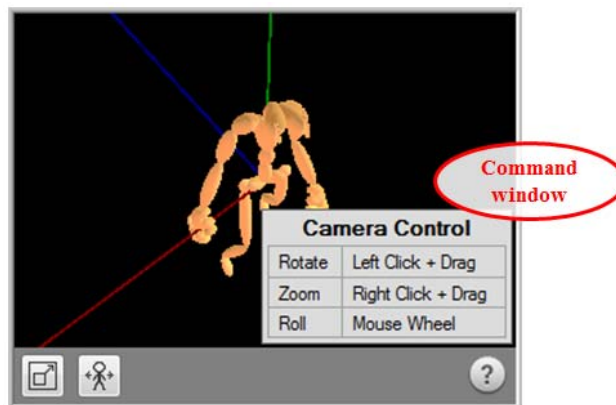


Figure 10. Motion capture panel with second model type and camera control dialog displayed

6. Biomechanical Data Graph Panel

A graphing window for plotting biomechanical data derived from motion capture data is located below the play control panel at the bottom of the main window. It provides the user with a means of determining the joint stresses and strains that result from specific postures and motions. The biomechanical data graph panel is shown in Figure 11.

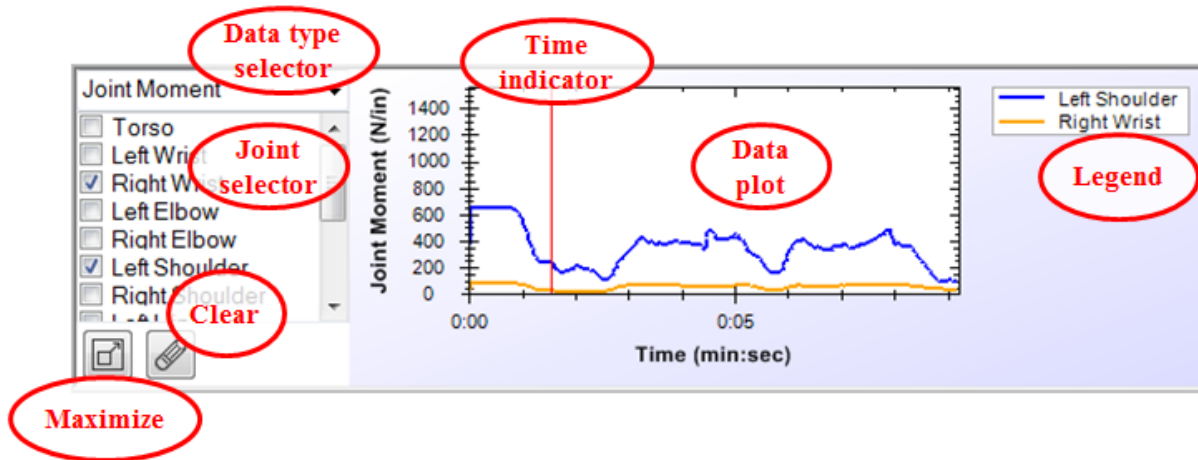


Figure 11. Biomechanical data graph panel

At the top-left is a drop-down menu for selecting the type of data that will be graphed on the plot (e.g., joint moment or strength capability). Below the data type selector is a list of all the available joints for which the selected data type can be graphed. Clicking on a joint name will display a check box for that joint and graph its data on the plot. The number and types of data and joints that are available for plotting will depend on the source of the biomechanical data.

To the right of the data type and joint selector menu is the data plot. It displays the biomechanical data for each selected joint. A legend at the top-right corner of the plot indicates the line color for each plotted joint. The plot's Y-axis is labeled with the type of data being graphed and the units for that data type. The X-axis is always labeled with the time, with 0:00 corresponding with the first frame of the video and motion capture files. A vertical red line on the data plot provides a visual indication of the current point in time being displayed in the video and motion capture panels.

The data plot can be panned by left-clicking inside the plot and dragging the mouse left or right. You can zoom in on the data plot by rotating the mouse wheel up or down. This allows you to isolate a smaller time segment for analysis, which is especially useful for longer motion sequences.

The button at the bottom-left corner of the panel maximizes the viewing window. The button to its right clears all of the selected joints and returns the graph to its initial launch state.

7. Human Body Diagram Panel

To the far-right side of the field tool's main window is the human body diagram panel, shown in Figure 12. It provides visual cues as to the magnitude of instantaneous joint stress levels, regardless of whether those joints are plotted in the biomechanical data graph.

The specific type of joint stress (e.g., joint moment or strength capability) for which the stress levels are indicated in the human body diagram panel is determined by the type of biomechanical data being plotted (see Section 6, Biomechanical Data Graph Panel: data type selector).

Stress levels are represented by ovals located at each joint for which biomechanical data is available. The colors of these ovals change from green (within normal tolerances), to yellow (within cautionary tolerances), to red (beyond maximum tolerances). The level ranges for each indication color are predetermined and dependent on the type of data being indicated. The number of joints for which indicators are available is dependent on the source of the biomechanical data—any joint that can be plotted in the biomechanical data graph panel for the selected data type will have a color-coded indicator displayed for it in the human body diagram panel.

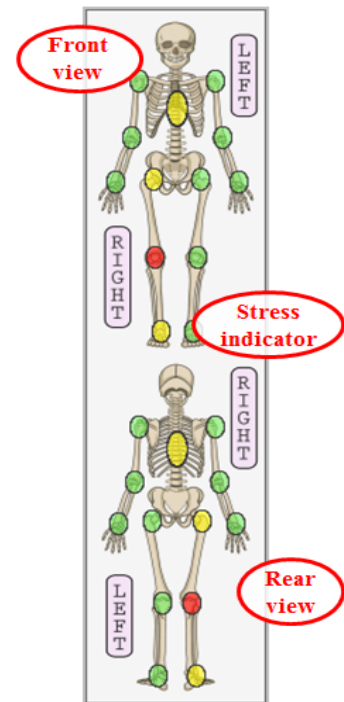


Figure 12. Human body diagram panel

8. Tips for Making Effective Use of the Field Tool

The field tool does not provide the user with instructions on how use the biomechanical and kinematic data presented. It is the user's responsibility to understand what these data mean and how they should be interpreted. Rather, the field tool simply provides a means for synchronizing and displaying data generated by marker-less motion capture biomechanical analysis processes. However, there are some helpful tricks for making the best use of the tool.

Keep in mind the adage “bad data in, bad data out.” The field tool does not provide any tools for evaluating the integrity of the loaded data. It is up to the user to ensure that each video, motion capture, and biomechanical data file loaded are from the same recording session and are temporally synchronized. Otherwise, any analysis made using the field tool will be erroneous.

During playback, keep an eye on the human body diagram panel. Watch for indicator color changes, particularly red colors that indicate maximum stress tolerance levels. For longer motion sequences, use the seek bar in the play control panel to pan the playback time from beginning to end. The human body diagram's indicator color shifts should be apparent. When one is noticed, concentrate on that time frame and analyze the video and motion capture data. Make sure the pose in the motion capture panel is an adequate representation of the posture of the subject shown in the video panel—if it's not, this indicates a problem during motion capture and any biomechanical data associated with that time frame should be disregarded. Keep in mind that the indicators in the human body diagram are associated with the type of biomechanical data being graphed.

When focusing on specific postures and movements, try pausing the files using the button at the center of the playback control panel. Select a data type and any joints of interest you would like to analyze in the biomechanical data graph panel. In the data plot, zoom in on the time frame where the pose and/or movement of interest is taking place (see Section 6, Biomechanical Data Graph Panel). Then, use the seek bar beneath the play/pause button to move the playback time back and forth along the time frame of interest. The vertical red bar in the biomechanical data graph plot will move, indicating the time period being displayed with sub-second accuracy. Analyze the postures taken by the recorded subject in the motion capture panel by rotating and zooming the camera (see Section 5, Motion Capture Panel). Use the biomechanical data graph to determine how specific motions and poses impact the stress levels at particular joints.

9.2 Dissemination: Journal Papers and Conference Proceedings

Journal Paper

- Seo, J., Starbuck, R., Han, S., Lee, S. and Armstrong, T. (2014). "Motion-Data-driven Biomechanical Analysis during Construction Tasks on Sites." Journal of Computing in Civil Engineering, ASCE, Reston, VA. (Invited Paper from article at the 2013 ASCE International Workshop on Computing in Civil Engineering: Submitted)

Conference Proceedings (with Presentation)

- Seo, J., Han, S., Lee, S., and Armstrong, T. J. (2013). "Motion-Data-driven Unsafe Pose Identification through Biomechanical Analysis." Proceeding of 2013 ASCE International Workshop on Computing in Civil Engineering, Los Angeles, CA. (Identified as one of the top papers and invited to the special issue publication in the ASCE Journal of Computing in Civil Engineering).
- Seo, J., Han, S., Armstrong, T. J., and Lee, S. (2013). "Force Prediction during Ladder Climbing for Biomechanical Analysis." Proceedings of the 8th International Conference on Prevention of Work-related Musculoskeletal Disorders, Busan, Korea.
- Han, S., Lee, S. and Armstrong, T. (2013). "Markerless Motion Tracking to Study Physical Stresses during Climbing." International Digital Human Modeling Symposium, Ann Arbor, MI.
- Seo, J., Lee, S., Armstrong, T. J., and Han, S. (2013). "Dynamic Biomechanical Simulation for Identifying Risk Factors for Work-related Musculoskeletal Disorders during Construction Tasks." Proceedings of the 30th International Symposium on Automation and Robotics in Construction and Mining (ISARC), Montréal, Canada.
- Seo, J., Han, S., Lee, S., and Armstrong, T. J. (2014). "Feasibility of On-Site Biomechanical Analysis during Ladder Climbing." 2014 ASCE Construction Research Congress. (Accepted).
- Starbuck, R., Seo, J., Han, S., and Lee, S. (2014). "A Stereo Vision-based Approach to Marker-less Motion Capture for On-Site Kinematic Modeling of Construction Worker Tasks," Joint Conference International Conference on Computing in Civil and Building Engineering and CIB W078 Annual International Conference, Orlando, Florida (Accepted).

- Seo, J., Starbuck, R., Han, S., Lee, S., and Armstrong, T. J. (2014). “Dynamic Biomechanical Analysis for Construction Tasks Using Motion Data from Vision-Based Motion Capture Approaches,” Joint Conference International Conference on Computing in Civil and Building Engineering and CIB W078 Annual International Conference, Orlando, Florida (Accepted).

9.3 Dissemination: Seminars

- Lee, S. (2013) “Markerless Motion Capture Approach for Unsafe Action Detection and On-Site Biomechanical Analysis” Department of Industrial and Operations Engineering, University of Michigan, Ann Arbor, MI.
- Lee, S. (2013) “Understanding the Human Aspects of Construction” Seoul National University (Joint Seminar for Seoul National University, Korea University, Ewha Womans University, and Kwangwon University), Seoul, Korea.
- Lee, S. (2013) “Understanding the Human Aspects of Construction” University of Seoul, Seoul, Korea.
- Lee, S. (2013) “Understanding the Human Aspects of Construction” Yonsei University, Seoul, Korea.
- Lee, S. (2013) “Understanding the Human Aspects in Built Environment” KyoungHee University, Suwon, Korea.
- Lee, S. (2013) “Understanding the Human Aspects of Construction” ChoongBook National University, CheongJoo, Korea.
- Lee, S. (2013) “Automatic Detection of Unsafe Actions in Construction: Markerless Motion Capture Approach” Occupational Health Speaker Series, School of Public Health, University of Michigan, Ann Arbor, MI.

